

Geodynamic regionalization of the recent structure of North Eurasia

A. F. Grachev, M. K. Kaban, and V. A. Nikolaev

Schmidt United Institute of Physics of the Earth, Russian Academy of Sciences

Abstract. Correlation analysis of geological and geophysical parameters of the North Eurasia lithosphere is performed on the basis of data for the recent vertical tectonic movements of the crust reflected in the 1:5 000 000 North Eurasia map of recent tectonics [*Neotectonic map...*, 1996] and calculated curvature intensities of the recent movements K_{int} , as well as such geophysical parameters as the heat flow HF, Moho depth, maximum and minimum tangential stresses $S_1 - S_3$ estimated from gravity data, and mantle anomalies with wavelengths shorter than 2400 km. The correlation analysis is complemented with factor analysis. Factors responsible for geodynamic regimes of North Eurasia are identified and mapped. They are used for the identification and interpretation of geodynamic classes of the lithosphere. Seismically active regions such as orogens, rifts and prerifts are examined separately; an additional parameter, the seismic activity A_{10} is used for this purpose. Aseismic platforms are also studied separately using, as a parameter, the crystalline basement depth instead of the seismic activity. Results of the geodynamic regionalization of seismically active and aseismic areas in North Eurasia are summarized in a general map of geodynamic regionalization of North Eurasia. Its analysis provided several constraints on the development and controlling factors of the majority of regions. Implications of the inferred results for the determination of tectonic stress fields are discussed.

Introduction

The problem of geodynamic regionalization cannot be solved without invoking various geological, geophysical and, as became clear recently, isotopic-geochemical data. The latter are helpful for interrelating data of chemical geodynamics and seismic tomography, and this in turn can provide constraints on depths of processes controlling the neotectonic activity.

Examples of regionalization of a single parameter are well known (for example, the folding age or the amplitudes of neotectonic movements in geotectonics). Such maps can be regarded as analytical in contrast to synthetic maps based on the analysis of a set of properties or parameters.

The construction of geodynamic regionalization maps involving a set of parameters requires the development of adequate methods and examples of such studies are few in modern literature. As was shown in [Grachev, 2000; Grachev *et al.*, 1989, 1992, 1995a, 1995b], a key aspect of this problem is the choice of initial parameters describing a geodynamic regime.

In choosing parameters, we used a method based on the factor analysis allowing one to select geological and geophysical data that make a significant contribution to the total variability. The method of principal components of the factor analysis is optimal for such a procedure.

For both objective (the nature of a structure studied) and subjective (the state of knowledge) reasons, the geodynamic regionalization of North Eurasia cannot be accomplished on the basis of indicative parameters that are the same throughout its territory. Thus, whereas such an important factor as seismic activity is usable in active regions, stable blocks of the lithosphere (ancient and young platforms) are virtually aseismic. Various regions also differ in the amount of information available on their fields (primarily, heat flow and a number of others). Finally, such a large territory as North

Copyright 2004 by the Russian Journal of Earth Sciences.

Paper number TJE04145.

ISSN: 1681–1208 (online)

The online version of this paper was published 27 May 2004.

URL: <http://rjes.wdcb.ru/v06/tje04145/tje04145.htm>

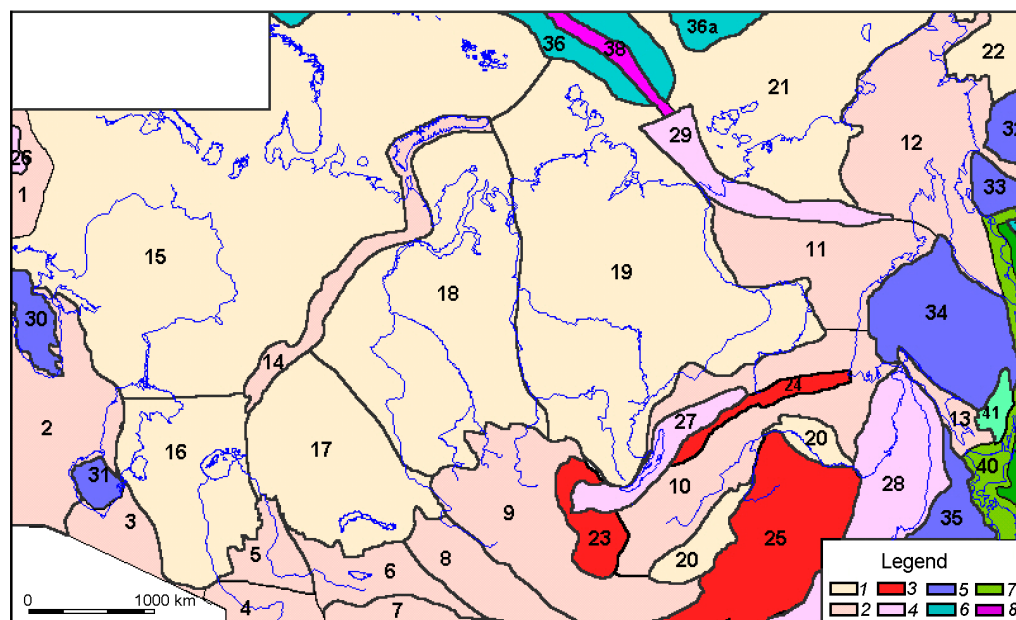


Figure 1. Map of active (neotectonic) geostructural areas of Northern Eurasia: I – Mountain-Building Areas: 1 – Carpathians, 2 – Caucasus, 3 – Kopet-Dag, 4 – Pamir-Alay, 5 – Southern Tien Shan, 6 – Northern Tien-Shan, 7 – Tarim Basin, 8 – Jungaria, 9 – Altai-Sayan-Mongolian, 10 – Mongolo-Okhotskaya, 11 – Verkhoynsko-Kolymskaya, 12 – Chukotskaya, 13 – Sakhakinskaya, 14 – Urals; II – Platform Areas: 15 – East-European, 16 – Turan, 17 – Kazakh shield, 18 – West Siberian, 19 – Siberian, 20 – Zeisko-Bureinskaya and Gobi-Xinganskaya, 21 – East Siberian-Chukotkian, 22 – Beringian; III – Prerift Areas: 23 – East Sayan, 24 – Vitim-Stanovoi, 25 – North-East China; IV – continental rifts: 26 – Pannonian, 27 – Baiklial, 28 – East Asian, 29 – Moma; V – Deep-Sea Basins: 30 – Black Sea, 31 – South Caspian, 32 – Bering Sea, 33 – Komandor basin, 34 – Okhotsk Sea, 35 – Japan Sea; VI – Oceanic Plates: 36 – Eurasian, 36a – Amerasian, 37 – Pacific; VII – Oceanic Rifts: 38 – Gakkel Ridge, VIII – Island Arcs: 39 – Kuril-Kamchatka deep-sea trench, 40 – Island arc, 41 – Backarc basin.

Eurasia has been studied very irregularly: data on the deep structure of several vast areas (e.g. northeastern Eurasia) are virtually absent. For these reasons, the geodynamic regionalization of North Eurasia was performed separately for stable and active blocks, after which results of these studies were joined together to form a general map.

Initial Data and Their Characterization

In constructing the 1:5 000 000 map of neotectonics of North Eurasia [*Neotectonic map...*, 1996], a geological-geophysical database of main parameters characterizing recent geodynamic settings was created. Major geostructural regions identified from analysis of neotectonic evidence are shown in Figure 1. As seen from this figure, a considerable part of the North Eurasia territory consists of stable lithospheric blocks (ancient and young platforms) variously inheriting ancient structural patterns [*Neotectonics...*, 2000].

In this paper, we address only the continental part of North Eurasia; the geological and geophysical parameters chosen for its analysis are presented in Table 1. Some of

these parameters were determined on the basis of pertinent maps (neotectonic movements, the density of faults from results of interpretation of satellite images, and etc.; see the CD application of [*Neotectonics...*, 2000]), whereas others were determined by converting various initial data (seismotectonic strain values, mantle gravity anomalies, and others [*Neotectonics...*, 2000]). All data were digitized in $20' \times 30'$ cells.

As mentioned above, a general approach to the geodynamic regionalization of the entire territory of North Eurasia cannot be implemented due to marked differences between the properties of stable and active regions; therefore, the geodynamic regionalization of these regions is carried out using parameters that were selected for this purpose on the basis of correlation and factor analyses.

Seismically Active Regions

Seismically active regions include orogenic areas, continental rifts, and prerifting zones [*Neotectonics...*, 2000]. These regions were analyzed on the basis of the following seven parameters:

Table 1.

w , amplitude of recent vertical movements (km)	Grad, gradients of recent vertical movements, (m/km)
K_{int} , curvature intensity of recent vertical movements, (km^{-1})	Moho, Moho depth (km)
T_{Moho} , temperature at the Moho surface ($^{\circ}\text{C}$)	HF, heat flow (mW/m^2)
$S_1 - S_3$, maximum tangential stresses in lithosphere (MPa)	S_v , vertical stresses in crust (MPa)
ISO, isostatic gravity anomalies (mGal)	A_{10} , seismic activity
b , earthquake recurrence plot slope	RESLOC, resulting local gravity anomalies (mGal)
RESREG, resulting regional gravity anomalies (mGal)	h_b , depth to the consolidated basement (km)
M_{Anom} , mantle gravity anomalies (mGal)	MAn2400, mantle gravity anomalies with a wavelength shorter than 2400 km (mGal)
H_{350} , Earth's magnetic field measured by satellites at an altitude of 350 km (Oe)	

- w , amplitude of recent vertical crustal movements (RVCM);
- K_{int} , RVCM curvature intensity;
- $S_1 - S_3$, maximum tangential stresses in lithosphere;
- MAn2400, mantle gravity anomalies with a wavelength shorter than 2400 km;
- Moho, Moho depth;
- HF, heat flow;
- A_{10} , seismic activity.
- The parameters K_{int} , $S_1 - S_3$, and MAn2400 are determined by calculations.

Neotectonic Movements, w

RVCM data provide important constraints on the tectonic evolution of a region studied. Based on these data, a 1:5 000 000 map of North Eurasia neotectonics was for the first time constructed [*Neotectonic map...*, 1996; *Neotectonics...*, 2000]. For the first time, this RVCM map showed, in terms of a unified legend, the neotectonic structure of continental North Eurasia and adjacent water areas. The map provides a general idea of the intensity and Neogene-Quaternary trends of the RVCM, as well as the RVCM distribution over the North Eurasia territory. The map shows continental and oceanic platforms, orogenic (mountain-building) areas, deep-sea basins, pririfting zones, island arcs, deep-sea trenches, and backarc basins [*Neotectonic map...*, 1996]. Data on neotectonic movements reflected in the map provide the opportunity of determining several geometric strain characteristics of the lithosphere over the period of its evolution under study [*Grachev*, 2000], which are used in the present work.

RVCM Curvature Intensity, K_{int}

The RVCM strain characteristics are of interest in many geodynamic and seismological applications: determination of the stress state of lithosphere, identification of spatial

seismicity patterns, the problem of crustal shortening, and so on. The curvatures of the bent lithosphere are advantageous over the RVCM amplitudes and gradients in that they are invariant under the motion of a lithospheric block as a rigid body and can therefore be linked to active tectonic stresses within the framework of correct geodynamic models.

It is not the amplitudes w proper but the characteristics of their relative variations in space that are of interest for analysis of the stress-strain state of lithosphere. These characteristics include the modulus of the RVCM amplitude gradient and the curvature of the RVCM induced surface. The relative variation characteristics of RVCM amplitudes are studied, in particular, in order to gain insights into the possible correlation between tectonic movements and seismicity. The problem of using RVCM data for seismic regionalization and earthquake prediction arose when sufficiently reliable data of observations became available. Bending deformations of tectonic movements were studied in [*Grachev et al.*, 1988, 1989, 1990] using the analysis of such scalar characteristics of the curvature as the mean and Gaussian curvatures. Later efforts were focused on more comprehensive incorporation of the RVCM kinematics, which required analysis of tensor characteristics of the surface bent by RVCM. Spatially nonuniform RVCM amplitudes w generally change the local curvature at an arbitrary point (x, y) of the Earth's surface. Given relatively small RVCM gradients characteristic, for example, of platform regions, such changes are described quite adequately by the curvature-torsion tensor $\nabla \otimes \nabla w$. The components of this symmetrical 2-D tensor of second rank are second-order spatial derivatives of the RVCM amplitudes $w(x, y)$.

In a linear approximation, eigenvalues of the curvature-torsion tensor are the principal curvatures $K_{\text{max}}(x, y)$ and $K_{\text{min}}(x, y)$ of the RVCM field; more specifically, these are the principal curvatures that would characterize an initially plane surface subjected to the action of the given RVCM field. The recent variation rates of the curvatures and the related velocities were estimated and mapped for the East European platform (EEP) in [*Grachev et al.*, 1995a, 1995b] on the basis of the analysis of torsion-curvature tensor. The determination of the RVCM-induced strain characteristics is relevant to many geodynamic and seismological applications: the determination of the stress state of lithosphere, the identification of spatial distribution patterns of seismicity, the problem of crustal shortening, and so on.

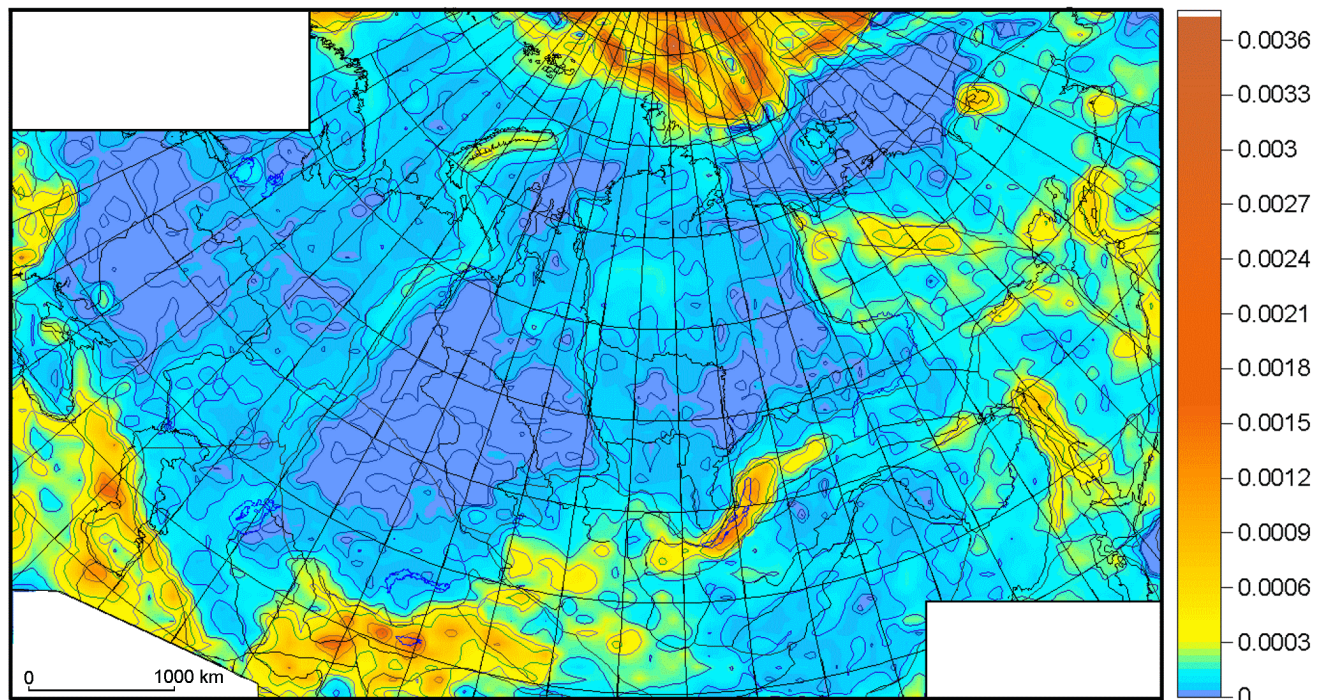


Figure 2. Intensity of bending (K_{int}) of neotectonic vertical movements.

If the thin plate bending model is adopted for the description of the lithosphere deformation, the stress state will be affected by all components of the tensor $\nabla \otimes \nabla_w$. They determine tensor characteristics of bending strain and therefore reflect regional and local disturbances of the global stress field transmitted from boundaries of lithospheric plates. Thus, within the model of small elastic bending deformations of an isotropic lithosphere, the torsion-curvature tensor is coaxial with the tensor of bending moments, the mean curvature K_{mean} is connected with disturbances of average stresses in the lithosphere plane, and the bending strain intensity defined as $h(K_{\text{max}} - K_{\text{min}})/2$ (h is the lithosphere thickness) affects the shear strain intensity and thereby the disturbance of the maximum tangential stress [Mukhamediev, 1992]. In bending models incorporating the inelasticity of deformations, anisotropy and layered structure of the lithosphere, the interrelation between the strain kinematics and stresses becomes more complicated but qualitatively remains basically the same.

The aforementioned properties of invariants of the tensor $\nabla \otimes \nabla_w$ were utilized to determine the spatial distribution of the bending strain intensity, estimate the rate of the EEP shear strain intensity, and compare it with the buildup rate of the seismic moment of earthquakes [Neotectonic map..., 1996]. The most interesting results were obtained for the Pannonian basin, where the localization of earthquake epicenters was found to be closely related to curvatures of neotectonic movements.

As was shown in [Grachev, 2000], the area-averaged curvature intensity K_{int} , defined as the half-difference modulus of principal curvatures and correlating (for certain types of regions) with the gradient modulus and principal curvature

moduli, is characterized by the least variation coefficient, as compared with any other geometric characteristics. This allows one to conclude that the area-averaged curvature intensity can be considered as a scalar characteristic providing the most reliable and adequate constraints on the deformation of most regions (Figure 2).

Mantle Gravity Anomalies

Density inhomogeneities in the upper mantle, associated with anomalies in the temperature field and chemical composition, provide one of the main driving forces of both vertical and horizontal movements of lithospheric blocks. Consequently, these inhomogeneities play a decisive role in geodynamic regionalization. On the other hand, the identification of mantle anomalies is a difficult problem. The observed gravity field includes the summarized effect of nearly all anomalous masses of the Earth and cannot therefore be used directly. The direct use of seismological data is also impossible because seismic velocities depend on many factors. The component produced by mantle density inhomogeneities should be extracted from the observed gravity field, and this problem cannot be solved without the construction of a density model of the crust.

The crustal density model of North Eurasia used in this paper is based on a synthesis on a large amount of information obtained by various geological and geophysical methods. Main stages of its construction are described in [Artemjev et al., 1994; Kaban, 2001, 2002]. Basic features of this model are briefly characterized below.

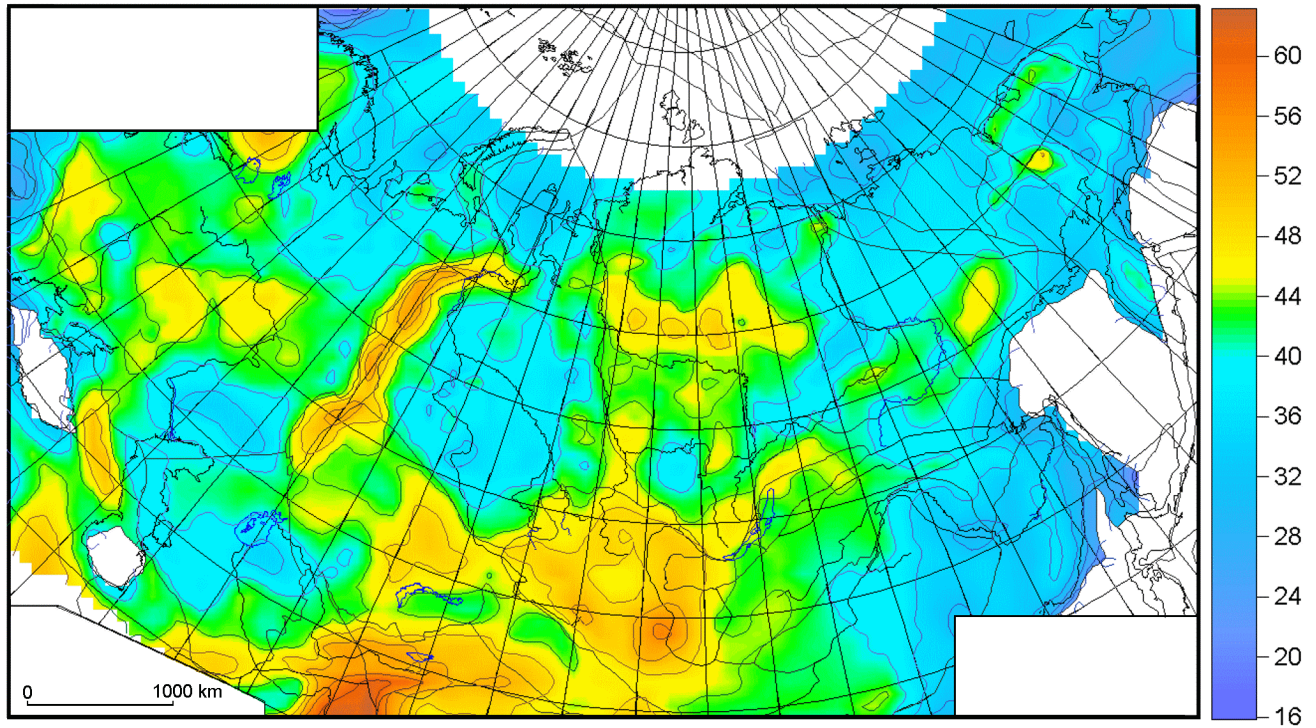


Figure 3. Moho boundary depths, km.

The total effect of density inhomogeneities of the sedimentary cover reaching -100 mGal, pertinent anomalies can be so extended that the low-frequency filtering methods, commonly used for the identification of the deep component, cannot suppress their effect. In order to determine the gravitational effect of sediments, maps of thickness and average density of the sedimentary cover were constructed in [Artemjev *et al.*, 1994]. These maps were updated in [Kaban *et al.*, 1998] to account for the results of later detailed studies including the information provided by Chinese geophysicists within the framework of a joint project [Feng *et al.*, 1996]. As a result, the gravitational field produced by sedimentary cover density perturbations relative to a constant density of 2.7 g/cm^3 was determined; the value 2.7 g/cm^3 can be regarded as a normal density of the upper part of solid crust in the absence of sediments. Supposedly, the determination uncertainty in this field does not exceed $10\text{--}15$ mGal for sufficiently extended structures (more than a few hundred kilometers in length). Of course, a large number of local sedimentary basins could not be accounted for in this study, but their effect is readily eliminated by low-frequency filtering.

A Moho topography map constructed through the synthesis of various geophysical (primarily, seismic) data is available for the territory studied [Artemjev *et al.*, 1994]. This map was updated with the use of data for Western Europe [Hurtig *et al.*, 1992], the Caucasus-Kopet Dag region and adjacent areas [Kaban *et al.*, 1998], Lake Baikal and adjacent areas (the pertinent map was prepared under the guidance of G. K. Levi at the Institute of Earth's Crust, Siberian Division of the Russian Academy of Sciences), and China

and Mongolia [Lithospheric..., 1989]. The updating was most significant for the territory of Russia; a map of Moho depths was constructed for this territory, except for northeastern Russia, under the guidance of S. L. Kostyuchenko at the GEON Center [Kostyuchenko *et al.*, 1999] (Figure 3). The anomalous gravitational field produced by variations in the Moho depth was calculated under the assumption that the density jump at the boundary is 0.43 g/cm^3 and does not change from region to region. This value of the difference between the average densities of the solid crust and upper mantle fits best the statistical relation between Moho depth variations and the near-surface load due to topography variations and the net effect of sedimentary cover density inhomogeneities [Artemjev *et al.*, 1994]. As a result, residual anomalies obtained after the removal of all effects related to crustal inhomogeneities and crustal thickness variations yields evidence on density variations in the lowermost crust and upper mantle, i.e. on zones in which the assumption on the homogeneity of the solid crust and upper mantle is violated.

The gravitational effect of solid crust density inhomogeneities was estimated on the basis of seismic velocity analysis [Kaban, 2001]. Seismic velocity variations were supposed to be directly related to density variations. Therefore, the reliability of this information is significantly lower compared to the data described above. This factor should be taken into account in analysis of mantle gravity anomalies, which are due in part to solid crust density anomalies that are either unaccounted for or misinterpreted.

After the gravitational effects of the sedimentary cover, Moho depth variations and solid crust density anomalies

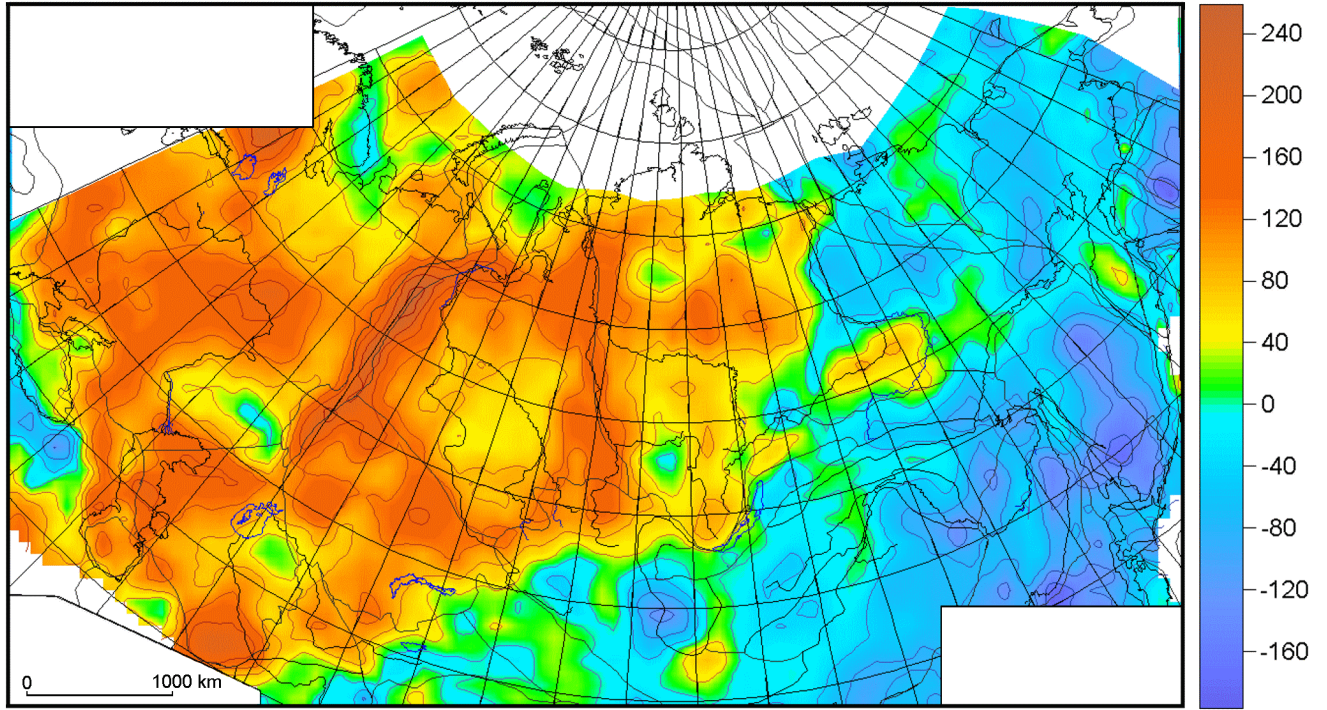


Figure 4. Gravity mantle anomalies, total field, mGal.

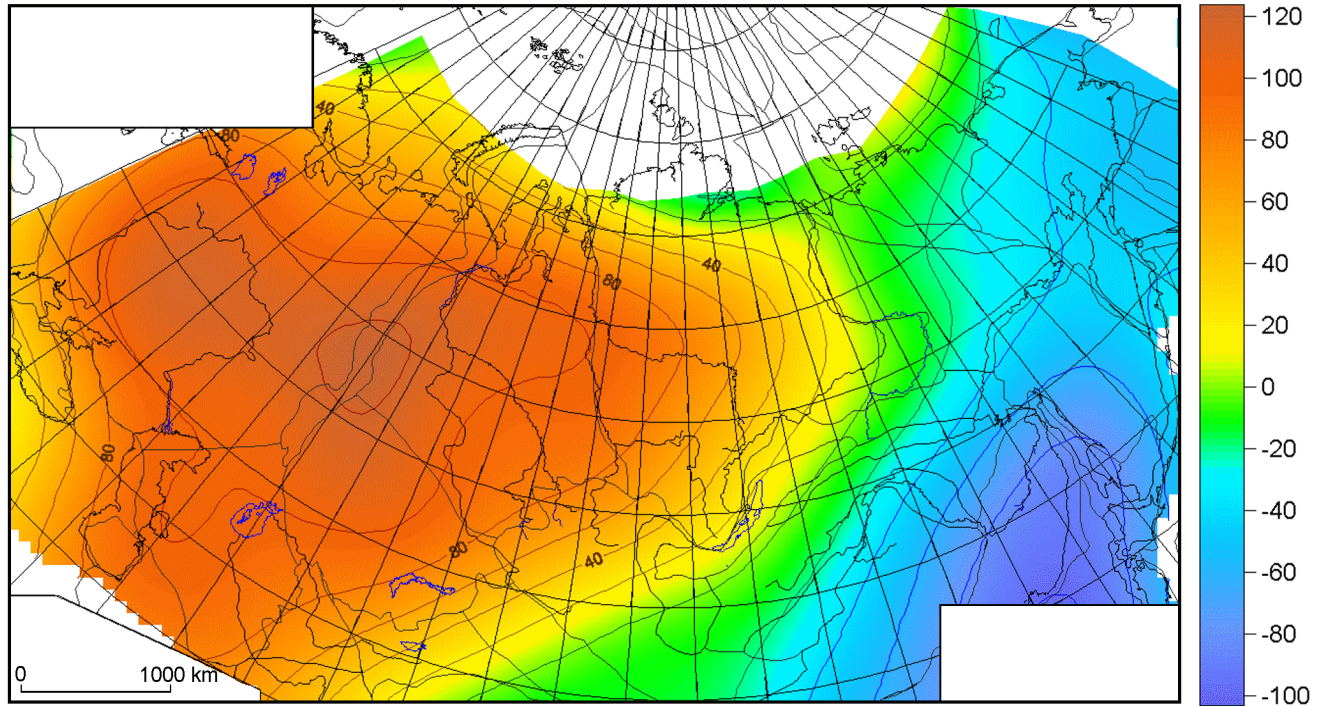


Figure 5. Gravity mantle anomalies with wave <2400 km, mGal.

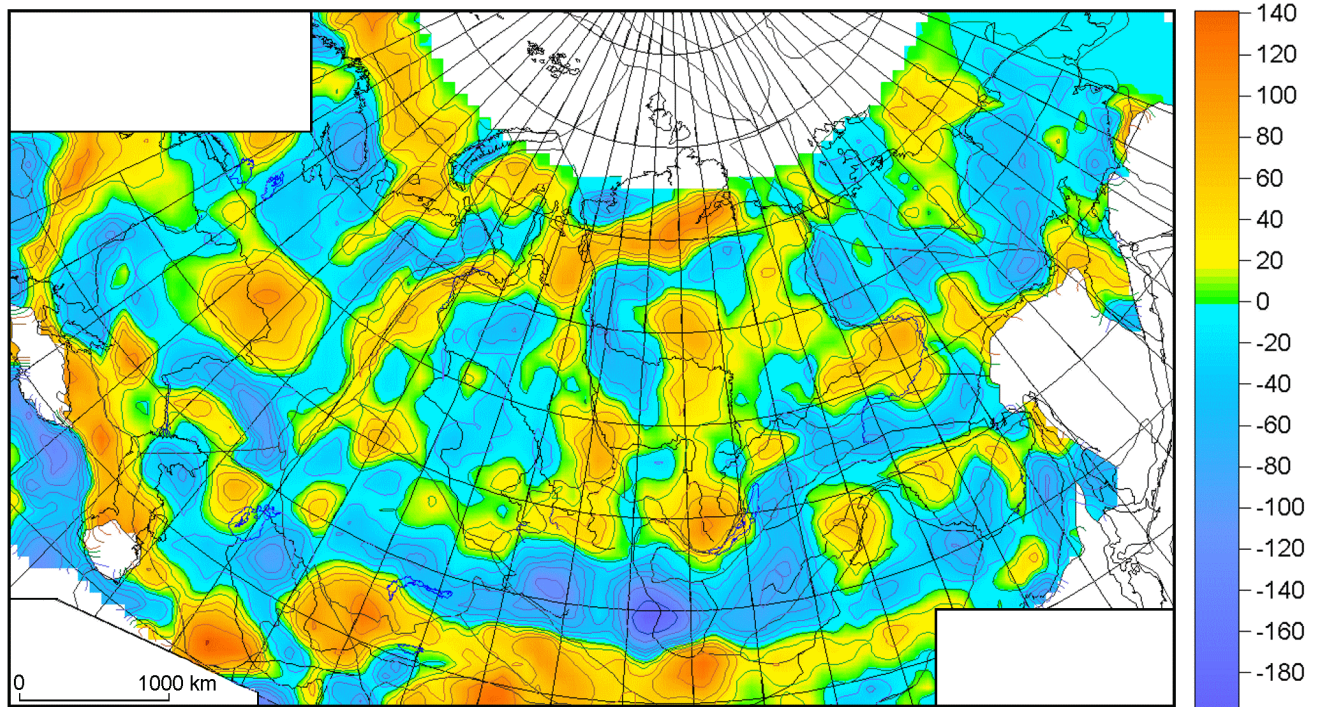


Figure 6. Gravity mantle anomalies, regional field, mGal.

were eliminated from the observed gravity field, residual anomalies of the mantle gravitational field were calculated. The mantle anomaly amplitudes in North Eurasia reach ± 250 mGal (Figure 4). The most remarkable feature of the inferred field is its distinct separation into regional (Figure 5) and local components. In a first approximation, the regional component is independent of variations in the crustal structure: vast areas dominated by anomalies of the same sign include fairly diverse structures. The northern and central parts of Eurasia are characterized by intense positive anomalies with average amplitudes of 100–150 mGal. Within North Eurasia, the regional component of the field of mantle anomalies is in good agreement with anomalies of the velocities V_s at depths greater than 100 km derived from observations of surface waves [Ritzwoller *et al.*, 1998]. This allows one to relate regional anomalies of the upper mantle density to the temperature distribution at the same depths. The horizontal dimensions of these anomalies agree with the sizes of main convective cells in the mantle obtained from numerical models [Trubitsyn, 2000; Trubitsyn and Rykov, 2000].

As distinct from the regional field, the field of residual anomalies with wavelengths shorter than 2000–2500 km displays a clear correlation with tectonic structures (Figure 6).

Local variations in mantle anomalies within platform areas are significantly smaller than in tectonically active zones. The most pronounced positive anomalies lie east of the Teisseyre–Tornquist line. For example, EEP shields are characterized by intense positive residual mantle anomalies

with amplitudes of up to +100 mGal. A similar anomaly is located in the western Urals (the Magnitogorsk zone). Mantle anomalies above the Tunguska syncline attain +100 mGal. This inference complies well with longitudinal wave velocities in the upper mantle (they are higher here). On the other hand, a chain of negative mantle anomalies is clearly traceable west of the Teisseyre–Tornquist line: Hungarian Plain–Rhine graben–French Massif Central. Noteworthy are intense negative mantle anomalies located along the eastern boundary of Eurasia and associated with marginal seas. Two well-developed zones of negative residual anomalies are recognizable in Central Asia. One of them is located southwest of Lake Baikal. This area, as well as a somewhat less developed area of negative anomalies near the northeastern end of Lake Baikal, may be classified as a hotspot. Another zone of intense negative mantle anomalies is located in the region of the Karakorum and Kun-Lun mountains at the boundary between the Tarim basin and Tibet.

Thus, the field of mantle anomalies with the removed long-wavelength component can be appropriately used for the purposes of geodynamic regionalization of North Eurasia. This field characterizes the geodynamics of the continent as a whole and largely masks anomalies of the subcrustal layer; the latter actually reflect the complicated evolution of various tectonic structures. The residual field characterizes lithospheric structures having lateral dimensions of up to 1500 km and is therefore relevant to the tasks of this study.

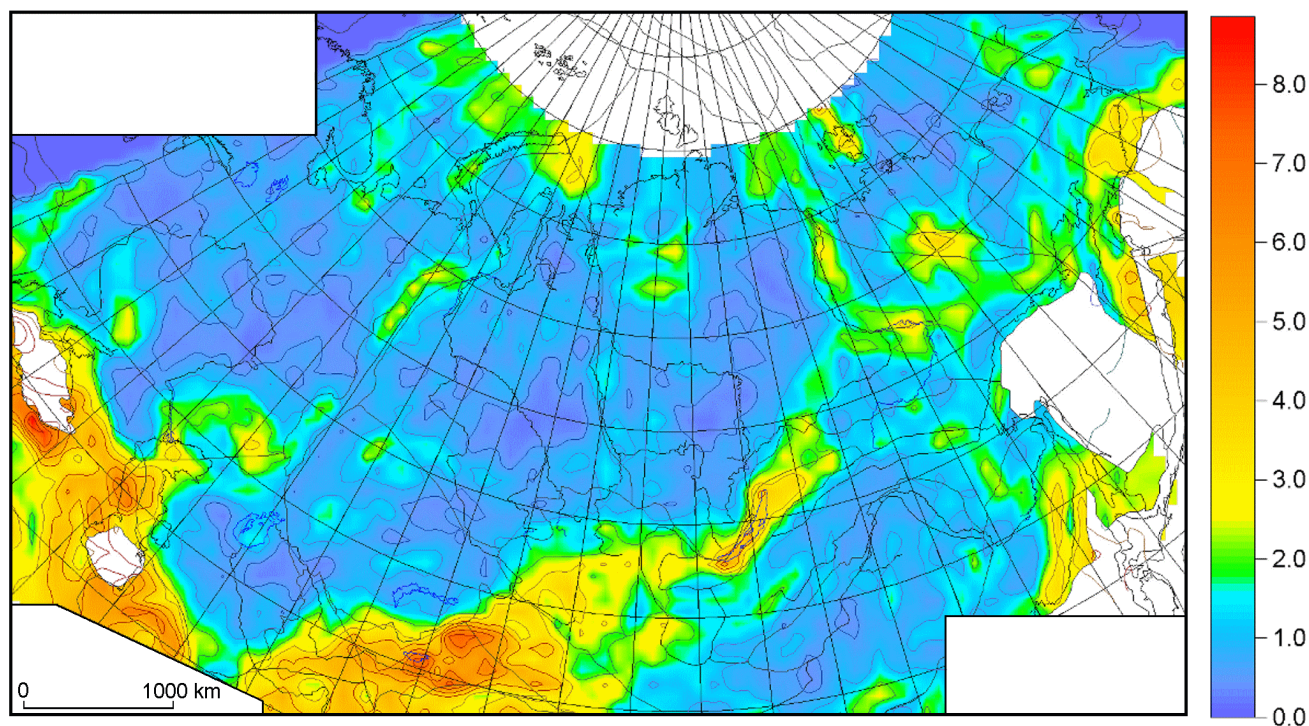


Figure 7. Maximum tangential stresses in lithosphere $S_1 - S_3$ (MPa).

Characteristic of the Stress State in the Lithosphere, $S_1 - S_3$

The stress state is one of the most important geodynamic characteristics of lithosphere. Comprehensive estimation of stresses is a complicated problem, which can only be solved in future. However, some qualitative estimates can be made even presently. The stress state of the lithosphere is controlled by several factors, which can be subdivided into two groups [Zoback *et al.*, 1992]. The first group includes factors related to the forces applied at the edges of lithospheric plates and to large-scale motions of mantle material. The related stresses are, as a rule, similar for large regions and are called regional stresses. Similarly to the case of long-wavelength mantle anomalies, the use of regional stresses for detailed geodynamic regionalization is ineffective.

The second group includes local (smaller-scale) stresses due to inhomogeneities of the structure and physical state in the crust and upper mantle (in particular, disturbances of the isostatic equilibrium). Artemjev *et al.* [1972] demonstrated theoretically that, even in an isostatically compensated lithosphere, amplitudes of local stresses due to density inhomogeneities can be of the same order as the maximum amplitude of regional stresses. Local stresses reflect a complex superposition of density inhomogeneities in the crust and upper mantle that are directly related to the dynamics of lithosphere.

Calculation of stresses in the upper crust utilizes a model in which a lithosphere resting on an effectively liquid substratum is represented as a set of elastic layers; elastic pa-

rameters within each layer are assumed to be constant, and the density varies laterally. This approach is described in detail in [Assameur and Mareshal, 1995; Kaban, 2001, 2003; Kaban and Yunga, 2000]. For our calculations, we used the density model of Eurasia developed in [Artemjev *et al.*, 1994; Kaban, 2001]. We should note that, although this model assuming elastic rheology is rather simple, the formulation of the problem admits considerably wider interpretation of its results, because the principle of correspondence between solutions obtained for elastic and viscoelastic bodies is valid in this case. Trial calculations showed that, in the upper 20 km, model stresses are largely insensitive to rheology variations at greater depths, which are determined less reliably.

This method was tested in the case study of the Baikal rift zone [Kaban and Yunga, 2000]. These authors showed that the distribution of model stress amplitudes at depths of 10–20 km in this region agrees with the distribution of earthquake sources. Thus, we may state that the model stresses adequately characterize one of the components of the complete stress field. Moreover, for the purposes of geodynamic regionalization, it is important to know stress concentrations in fairly extended areas rather than the values of the stress tensor at a given point, and our method is most effective and reliable precisely in this case. Even if main sources of the lithosphere stress state are associated with processes at plate boundaries (the Alpine-Mediterranean foldbelt is a case in point), these processes lead to anomalously high concentrations of density inhomogeneities at all levels, so that this method yields a plausible integral estimate. It is generally insignificant whether local density inhomogeneities produce anomalous stresses or are due to their effect; in both cases,

Table 2. Correlation matrix of seven geological-geophysical parameters of seismically active regions in North Eurasia

	w	K_{int}	$S_1 - S_3$	MAN2400	Moho	HF	A_{10}
w	1	-0.079	0.106	-0.317	0.371	0.035	0.018
K_{int}	-0.079	1	0.483	0.103	0.227	0.106	0.177
$S_1 - S_3$	0.106	0.483	1	0.017	0.335	-0.012	0.145
MAN2400	-0.317	0.103	0.017	1	0.120	-0.144	-0.085
Moho	0.371	0.227	0.335	0.120	1	-0.177	0.156
HF	0.035	0.106	-0.012	-0.144	-0.177	1	0.052
A_{10}	0.018	0.177	0.145	-0.085	0.156	0.052	1

the greater the density differentiation (beginning from the topography), the higher the stress estimates obtained by the method described above.

In this work, we used the estimates of local stresses in the upper crust of North Eurasia obtained in [Kaban, 2001, 2003]. Figure 7 presents values of the difference between the maximum and minimum values ($S_1 - S_3$) of the diagonal stress tensor T (the twofold maximum tangential stress $2\tau_{\text{max}}$); the tensor T was calculated at nodes of the $10' \times 15'$ grid at a depth of 12.5 km. The parameter $S_1 - S_3$ can be considered as one of the most general characteristics of the lithosphere stress state. As seen from Figure 7, values of this parameter reach 140 MPa, which agrees on the order of magnitude with maximum amplitudes of stresses estimated by seismic methods [Zoback *et al.*, 1992].

The model stress distribution in North Eurasia is consistent with the expected pattern: tectonically active areas correlate generally well with areas of higher τ_{max} values. However, significant variations are observable even within structures of the same type. Thus, orogenic zones are evidently divided into two types. The Caucasus, Kopet Dag, Pamirs-Altai and Tien Shan are distinguished by very high stresses, averaging 40 MPa and reaching 140 MPa. Substantially lower stresses (averaging 20 MPa and reaching 45 MPa) are observed in the Urals, Altai and Sayany. Platform regions are also separated in accordance with τ_{max} values. Maximum τ_{max} values are observed in East Siberia, and their minimum is located in West Siberia. The EEP is intermediate in this respect. This parameter was also included into the geodynamic regionalization scheme of North Eurasia.

Table 2 presents values of the correlation matrix of the seven selected parameters. Active regions are represented

by 11133 cells in which the parameters were quantified. As seen from the correlation matrix, the highest positive correlation is observed in the pairs ($S_1 - S_3, K_{\text{int}}$), (Moho, w), and ($S_1 - S_3, \text{Moho}$). We used factor analysis for examining the internal structure and internal relationships of the correlation matrix.

The first three components (factors) account for 63% of the total variability; the contributions of the 1st, 2nd and 3rd factors to the total variability are, respectively, 26.5, 20 and 17.4% (Table 3). Table 4 presents the factor loads of the initial parameters. The first factor of variability (26.5%) includes K_{int} , $S_1 - S_3$, and the seismic activity A_{10} and accounts for the stress state of lithosphere (Figure 8). The second factor relates the amplitude of neotectonic movements and short-wavelength mantle anomalies with opposite sign (Figure 9). In geodynamics, this is a rather long-lasting conservative factor accounting for slow neotectonic movements associated with processes in the mantle. The third factor relates the Moho depth and the heat flow with an opposite sign and accounts for the heating of the crust (Figure 10).

The three factors inferred for the territory of Eurasia are used as a basis for the geodynamic classification of seismically active regions in North Eurasia. For this purpose, we applied the classification method of K -averages. Table 5 shows the final centers of 15 classes calculated from the three factors. In applying the classification procedure, we used various numbers of *a priori* specified classes, from 10, 11 and 12 to 18, 19 and 20. Upon comparative analysis, we adopted 15 classes.

Table 6 presents the number of cells in each of the 15

Table 3. Eigenvalues of the correlation matrix (Table 2)

Components	Eigenvalues	Variations, %;	Total, %
1	1.857	26.523	26.523
2	1.400	19.996	46.518
3	1.220	17.424	63.942
4	0.908	12.966	76.909
5	0.751	10.734	87.643
6	0.475	6.782	94.425
7	0.390	5.575	100

Table 4. Factor matrix upon rotation

	Factors		
	1(26.5%)	2(20%)	3(17.4%)
w	0.336	0.873	0.174
K_{int}	0.820	-0.211	-0.05
$S_1 - S_3$	0.776	0.06	0.160
MAN2400	0.08	-0.674	0.468
Moho	0.469	0.376	0.617
HF	0.191	0.7	-0.772
A_{10}	0.467	0.125	-0.188

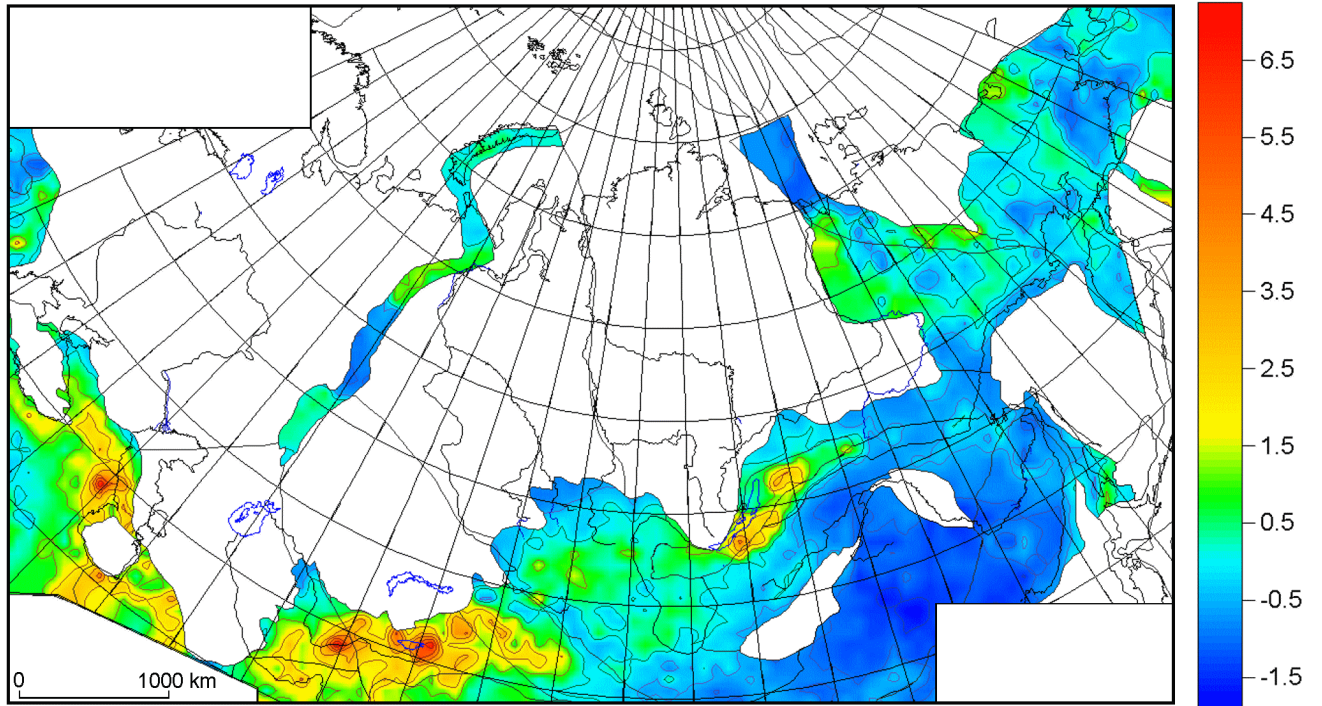


Figure 8. Map of factor 1 (A_{10} , K_{int} , $S_1 - S_3$).

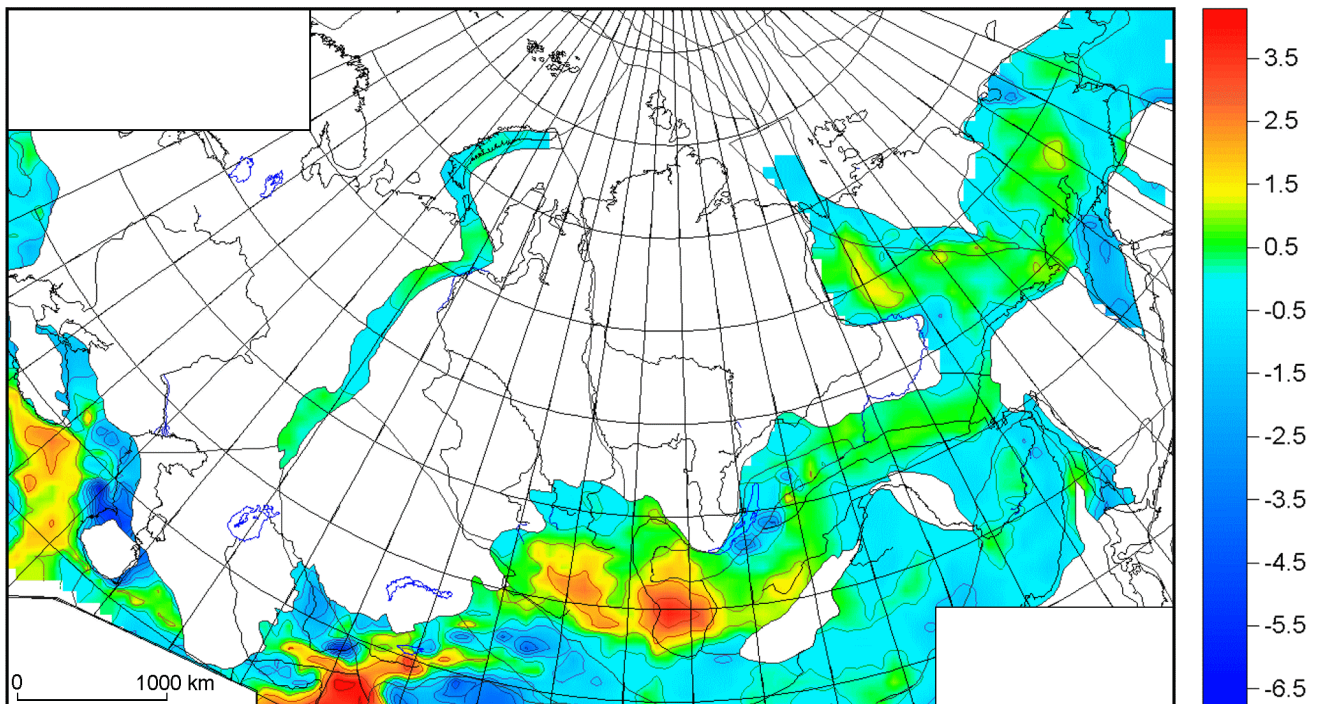


Figure 9. Map of factor 2 (w , MAn2400).

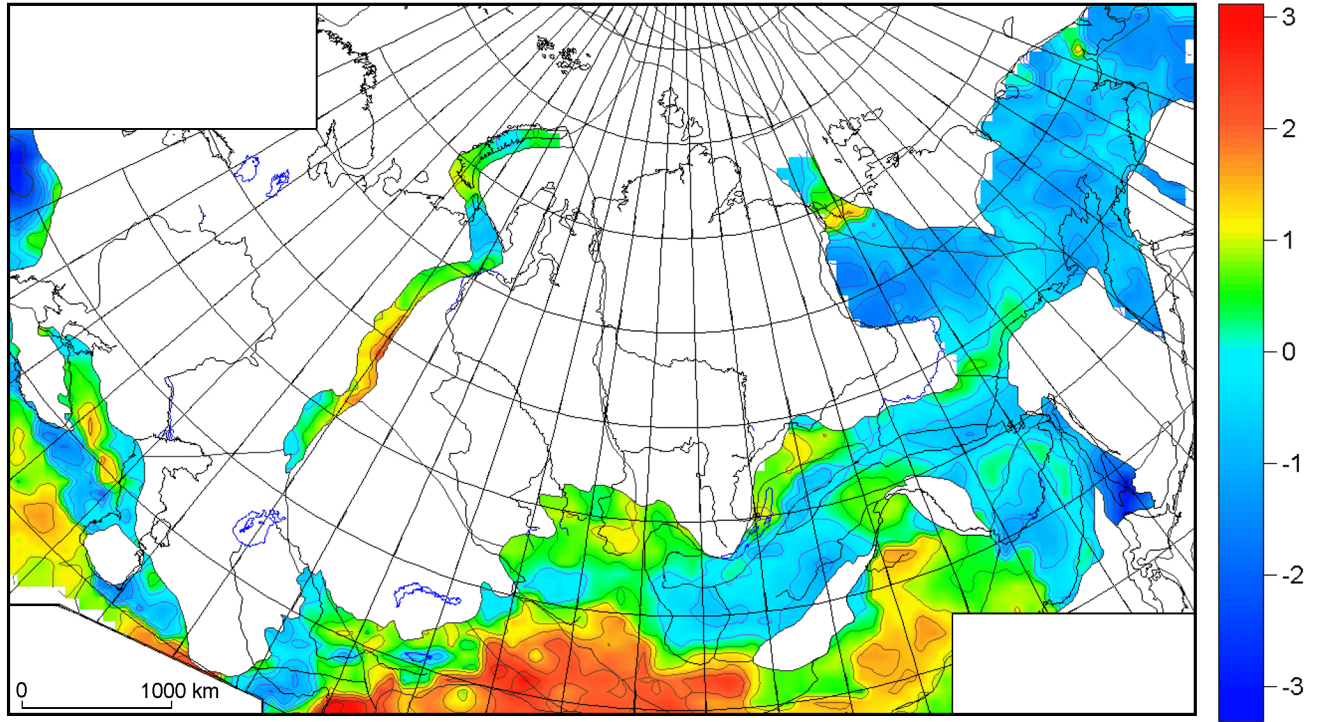


Figure 10. Map of factor 3 (Moho, HF).

classes. This number is smallest in the 7th class (63 cells) and largest in the 13th class (2000 cells).

The manual union procedure based on the taxonomical affinity is unnecessary. It should be applied if a compromise between detailedness and generalization is sought for. In our case, the 15 classes yielded overly mosaic pattern (Figure 11). To generalize this pattern, we examined the dendrogram of the taxonomical affinity of classes for the purpose of possible union of the closest classes such as (3, 5, 11, 13 and 4) and (6, 1 and 15). As a result, we obtained the regionalization scheme with 10 classes, shown in Figure 12.

Aseismic Stable Regions

Aseismic stable blocks of lithosphere include ancient and young platforms, which are characterized by 19 geological-geophysical parameters. Correlation analysis of these parameters showed that only seven of them are appropriate

for factor analysis (Table 7). The area under consideration consists of 15402 cells.

Analysis of the correlation matrix (Table 8) of the seven parameters reveals a strong positive correlation between Moho and neotectonic movements w and between $S_1 - S_3$ and Fund. The correlation coefficient is small between the maximum tangential stresses in lithosphere $S_1 - S_3$ and the curvature intensity K_{int} ; also small is the inverse correlation between Moho depths and the heat flow HF.

The first three components (factors) account for 62.24% of the total variability, and the contributions of the 1st, 2nd and 3rd factors are, respectively, 28.5, 18.7 and 15% (Table 9).

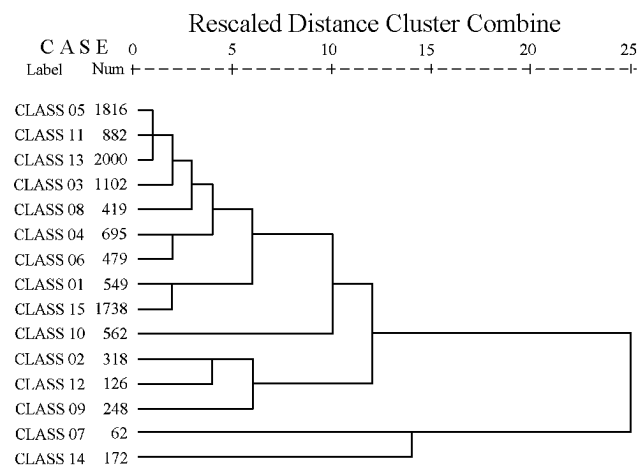
This factor model accounts for 62.24% of the total variability of the correlation matrix. The first factor includes the amplitude of neotectonic movements, Moho depth and heat flow with opposite sign and accounts for the recent deep heating of the upper mantle responsible for the observed neotectonic movements (Table 10, Figure 13).

The second factor includes the curvatures of neotectonic

Table 5. Classification in 15 classes by the method of K -averages: final centers of classes

	Classes														
	1	2	3	4	5	6	7	8	9	10	11	12	13	14	15
Factor 1	0.11	1.98	0.18	-0.01	-0.18	0.12	4.16	1.09	1.99	0.73	0.31	3.79	-0.72	1.28	-1.00
Factor 2	-0.61	0.41	0.52	-0.56	0.60	-1.51	-3.66	1.00	-1.10	2.33	-0.10	0.12	-0.18	-2.95	-0.31
Factor 3	1.83	1.22	0.69	-1.68	-0.80	-0.38	-0.62	-0.81	-0.56	0.59	-0.31	0.43	-0.35	1.16	0.91

Table 6. Dendrogram of crustal classes for seismically active regions of Eurasia, obtained by the method of averaged relationships between groups



movements characterizing, as is known, the stress state of the upper lithosphere and the maximum tangential stresses characterizing the stress state of the deeper lithosphere (on average, at depths of 12–25 km; see Figure 14).

Table 7.

w , amplitude of neotectonic movements
 K_{int} , curvature intensity of neotectonic movements
 $S_1 - S_3$, maximum tangential stresses in the crust
 MAn2400, short-wavelength (<2400 km) component of mantle gravity anomalies
 Moho, depth to the Moho
 HF, heat flow
 Fund, depth to the crystalline basement

Finally, the third factor interrelates short-wavelength mantle anomalies and the depth to the crystalline basement. This can be interpreted as evidence for mantle roots of crustal structures (Figure 15).

The inferred three factors were used for the classification by the method of K -averages. Initially, we determined 15

Table 9. Eigenvalues of the correlation matrix

Components	Eigenvalues	Variations, %
1	1.997	28.525
2	1.311	18.724
3	1.050	14.995
4	0.912	13.023
5	0.762	10.888
6	0.581	8.306
7	0.388	5.538

classes. Table 11 presents their final centers, which were used for constructing the classification dendrogram of the taxonomical affinity of lithospheric classes (Table 12).

Figure 16 shows 15 classes of the crust in platform regions derived from three factors by the classification method of K -averages. The map in Figure 16 being overly mosaic, we used the dendrogram of the taxonomical affinity of the 15 classes (Table 12) in order to unite some classes and thereby generalize this map. The dendrogram structure allowed us to unite taxonomically close classes 3, 5, 9 and 10; 4, 13 and 14; and 6 and 15. (Note that the numbers of cells in classes 3, 10 and 5 are very small: 10, 71 and 155, respectively.) The resulting map showing 9 classes is presented in Figure 17.

Table 10. Matrix of loads of main factors

	Factors		
	1(28.5%)	2(18.7%)	3(15%)
w	0.758	-0.02	-0.160
K_{int}	0.02	0.873	-0.08
$S_1 - S_3$	-0.225	0.709	0.235
MAn2400	0.173	-0.004	0.824
Moho	0.852	-0.03	0.202
HF	-0.598	0.185	0.08
Fund	-0.250	0.117	0.653

Table 8. Correlation matrix of 7 geological-geophysical parameters of platform regions

	w	K_{int}	$S_1 - S_3$	MAn2400	Moho	HF	Fund
w	1	-0.081	-0.192	-0.090	0.486	-0.273	-0.092
K_{int}	-0.081	1	0.311	0.044	-0.055	0.153	0.023
$S_1 - S_3$	-0.192	0.311	1	0.051	-0.165	0.150	0.268
MAn2400	-0.090	0.044	0.051	1	0.250	0.023	0.167
Moho	0.486	-0.055	-0.165	0.250	1	-0.330	-0.133
HF	-0.273	0.153	0.150	0.023	-0.330	1	0.125
Fund	-0.092	0.023	0.268	0.167	-0.133	0.125	1

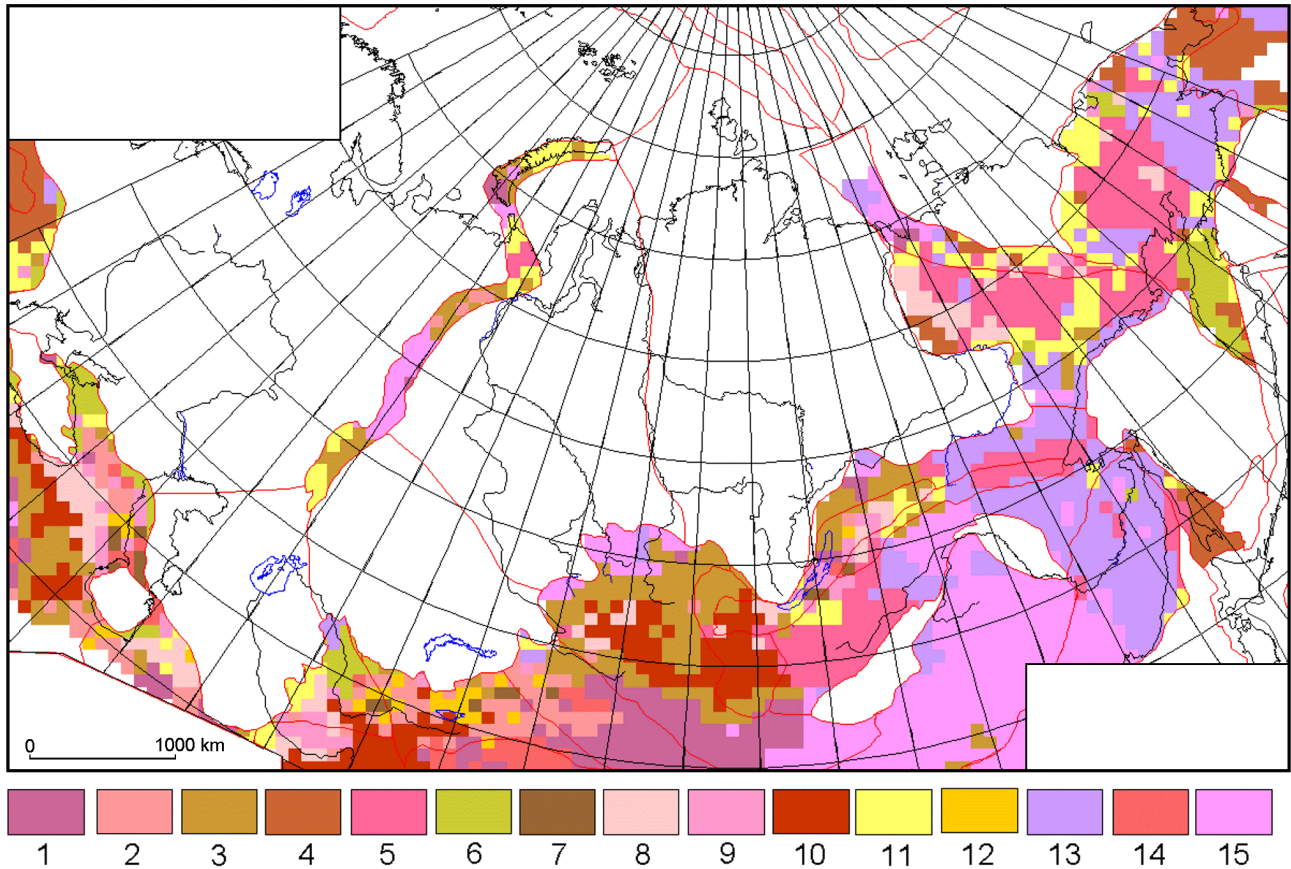


Figure 11. Classification of active areas. 15 classes.

Discussion and Conclusions

The final scheme summarizes results of geodynamic regionalization of North Eurasia obtained separately for seismically active regions and stable blocks of the lithosphere (Figure 18, Figure 19 – smoothed boundaries).

Platform regions. Class 1 is represented in the northern cis-Caspian depression, South Tura trench of the Turan plate, and Enisei-Olenek basin. The poorly developed class 2, occupying only 267 cells, is observed on peripheries of platforms, at their boundaries with orogenic areas. Classes 3, 5, 9 and 10, manually united into one class, also contain a small number of cells and occupy the eastern

Turan plate, Black Sea monocline, Central Yakutian basin and southern part of the Bering plate. The united classes 4, 13 and 14 occupy the largest area (5842 cells) and include a considerable part of the EEP, nearly entire Kazakh Shield, central and western Siberian platform, and Gobi-Khingian platform. The united classes 6 and 15 (1656 cells) include the Upper Lena, Enisei and Putorana inliers of the Siberian platform, Sur-Darya inlier and Chu-Muyunkum basin of the Kazakh Shield, and Aral-Buzuchan basin of the Turan plate.

In the EEP, these classes include the entire Upper Volga basin and the adjacent part of the Middle Russian inlier, as well as the Polish inlier. Class 7 occupies a large part of the Yamal-Gydan structural bench of the West Siberian plate and the northern part of the Bering

Table 11. *K*-average classification using 15 classes: final centers of classes

	Classes														
	1	2	3	4	5	6	7	8	9	10	11	12	13	14	15
Factor 1	-0.54	0.54	2.68	0.22	-3.69	0.96	-1.98	-0.22	-1.25	1.1	-0.46	-0.89	1.00	0.93	0.89
Factor 2	0.15	2.91	15.30	-0.52	2.30	-0.24	-0.375	-0.24	0.89	6.49	0.56	-0.48	-0.40	0.11	1.19
Factor 3	2.46	-0.47	-2.55	-0.54	-0.05	1.33	-0.265	0.53	0.95	-0.626	-1.11	-0.47	0.11	-0.99	0.58

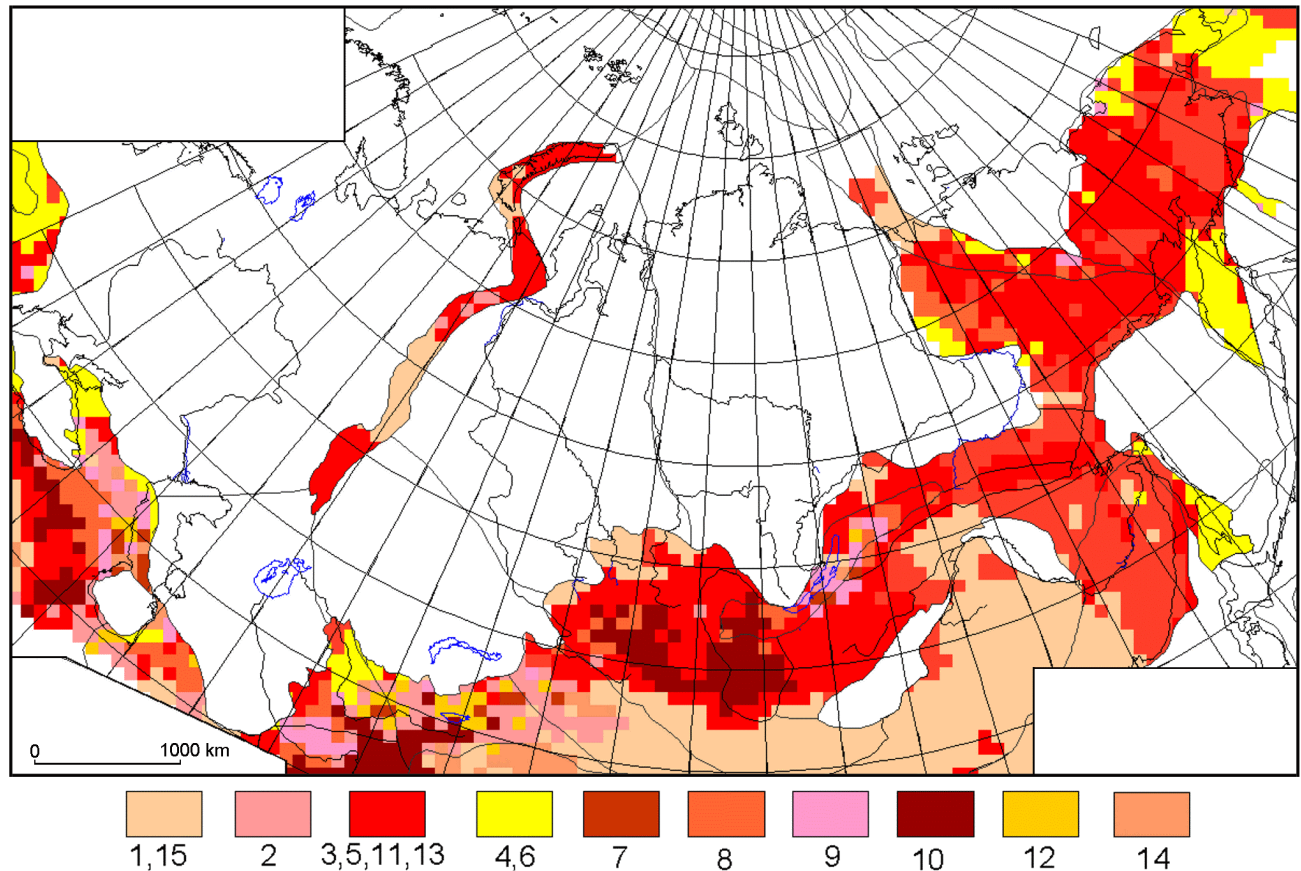
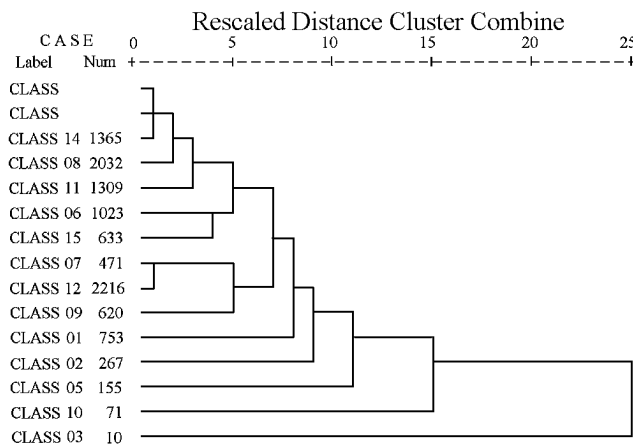


Figure 12. Classification of active areas. 10 classes.

plate. Class 8 includes the Pechora and Azov-Kuban basins, Elogii-Pakulikhinsk monocline, Lower Ob structural bench of the West Siberian plate, and the southern and northern parts of the Kan-Chona system of basins of the Siberian platform.

Table 12. Dendrogram of geodynamic classes of stable lithospheric blocks in North Eurasia obtained by the method of averaged relations between groups



Class 11 is rather widespread in the Turan plate, northern parts of the Mezen and Cis-Caspian basins of the EEP, and northern part of the East Siberian-Chukotka plate. Finally, class 12 is developed in the central part of the East Siberian plate, parts of the Karakum structural bench and Aral-Syr Darya saddle in the Turan plate, and the northern continental part of the East Siberian-Chukotka plate.

Overall, the EEP, Siberian Platform and Kazakh Shield are dominated by the crustal type defined by classes 4, 13 and 14. The crust of class 12 prevails within the East Siberian plate, and the Turan plate is distinguished by a complex mosaic structure dominated by classes 1, 2, 3, 5, 9, 10 and 12. Classes 2, 7, 8 and 11 are transitional and are not widely spread geographically.

We identified ten crustal classes characterizing seismically active areas. Class 1 is developed in 2289 cells and includes the nearly entire Northeastern China prerift zone, southern parts of the East Asian continental rift, and the Altai-Sayany-Mongolia orogenic area. Class 2, represented by only 318 cells, includes the Dzhungaria-North Tien Shan zone of orogeny.

The united classes 3, 5, 11 and 13 encompass a vast area consisting of 5800 cells. The crust of these geodynamic classes is widespread in the Trans-Caucasian region, the Southern and Northern Urals and New Land, as well as in the Chukotka, Verkhoyansk-Kolyma and Mongolia-Okhotsk

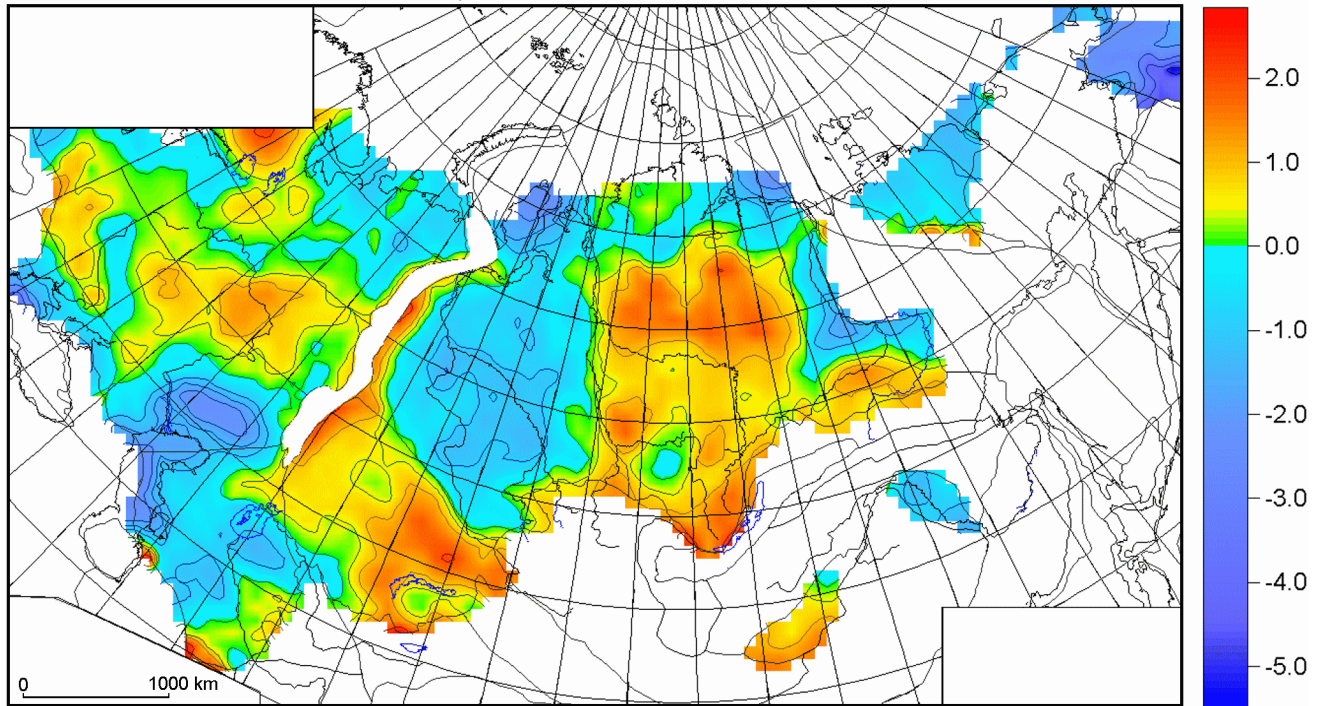


Figure 13. Map of factor 1 (w , Moho, HF).

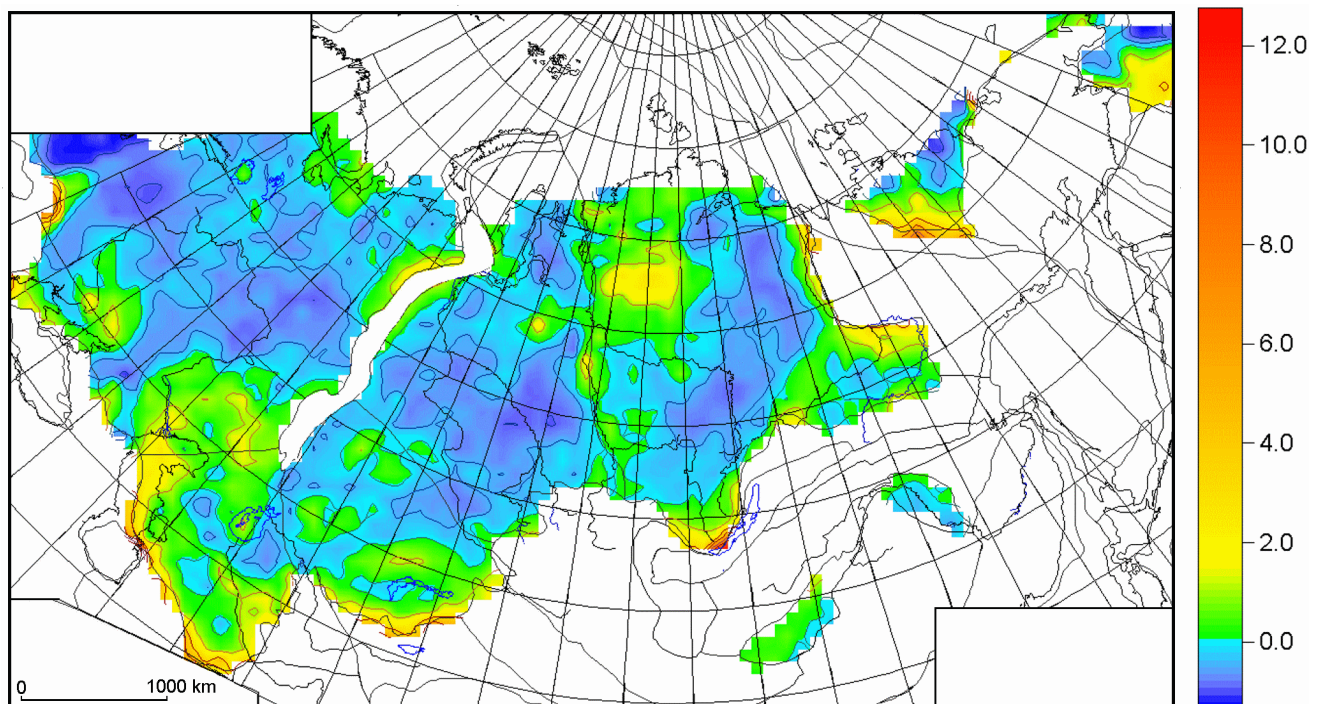


Figure 14. Map of factor 2 (K_{int} , $S_1 - S_3$).

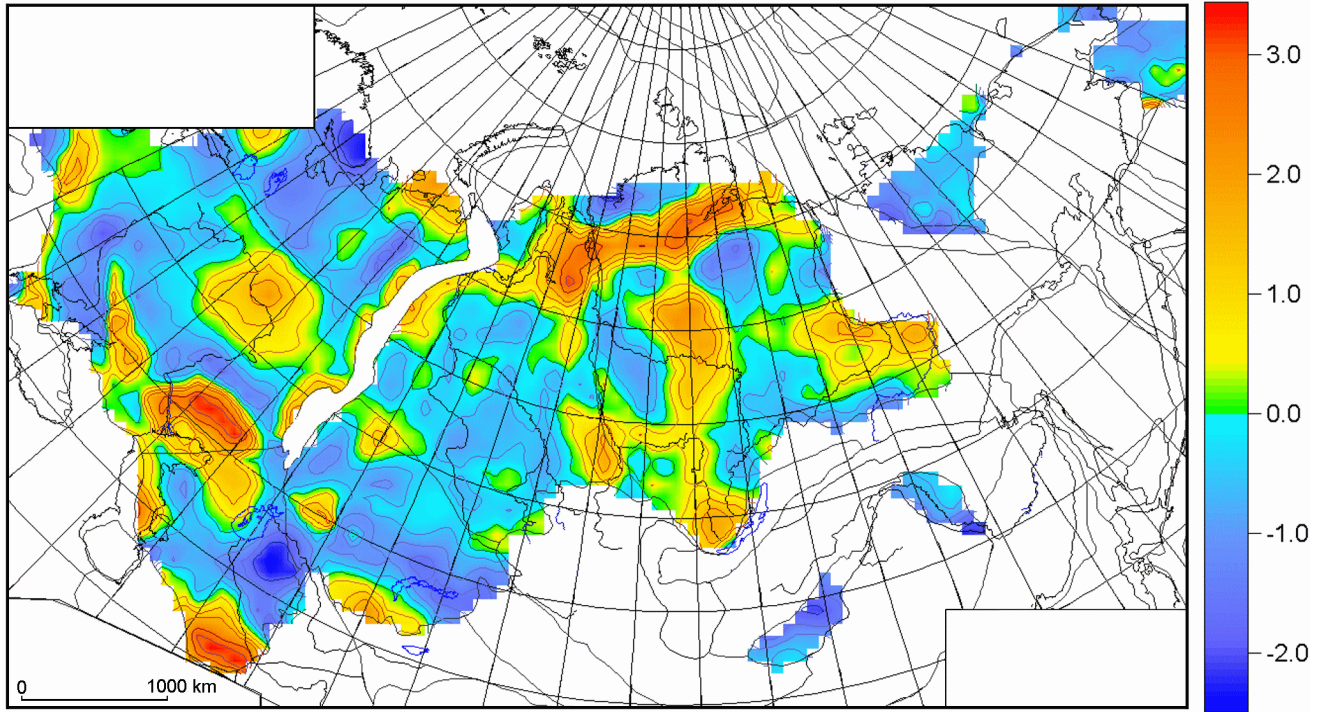


Figure 15. Map of factor 3 (MAan2400, Fund).

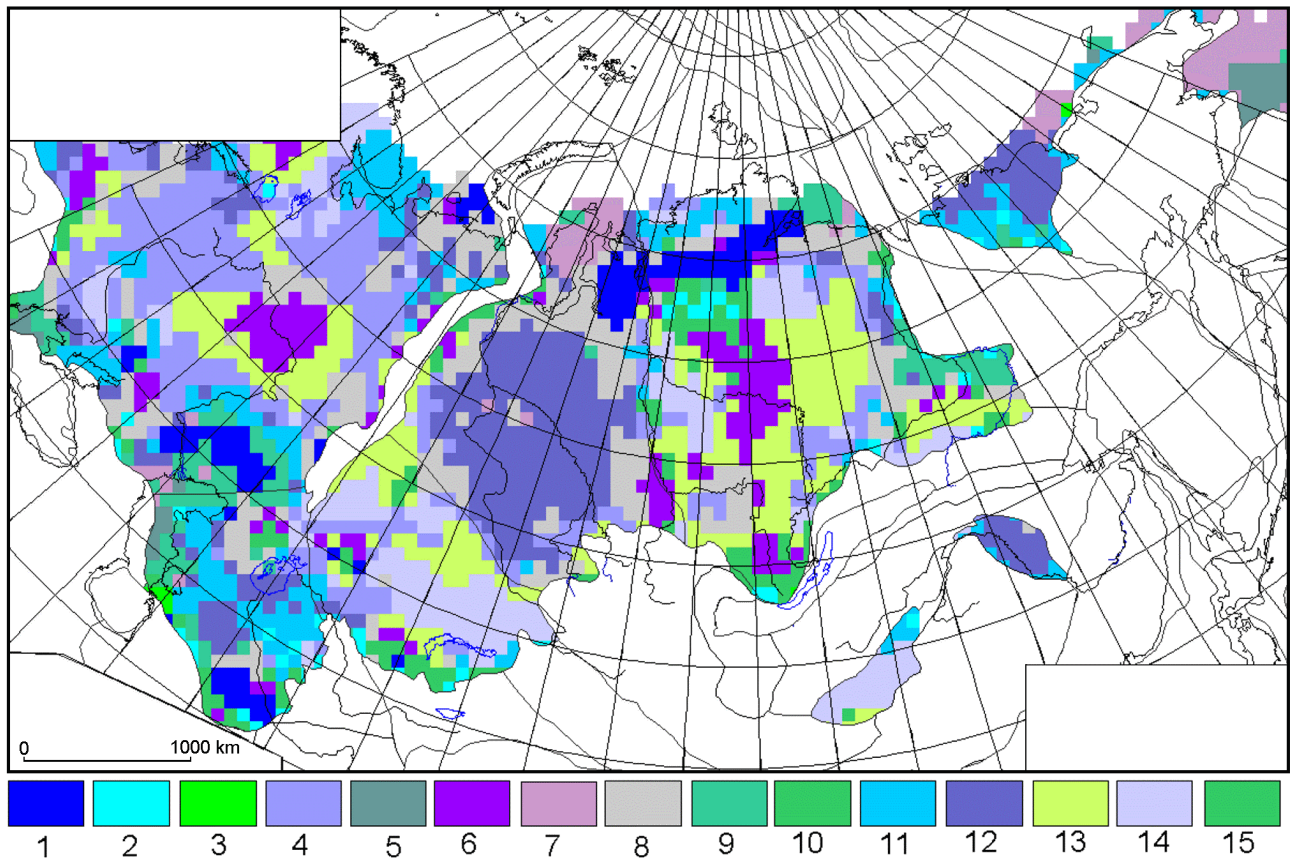


Figure 16. Classification of platform areas. 15 classes derived from three factors.

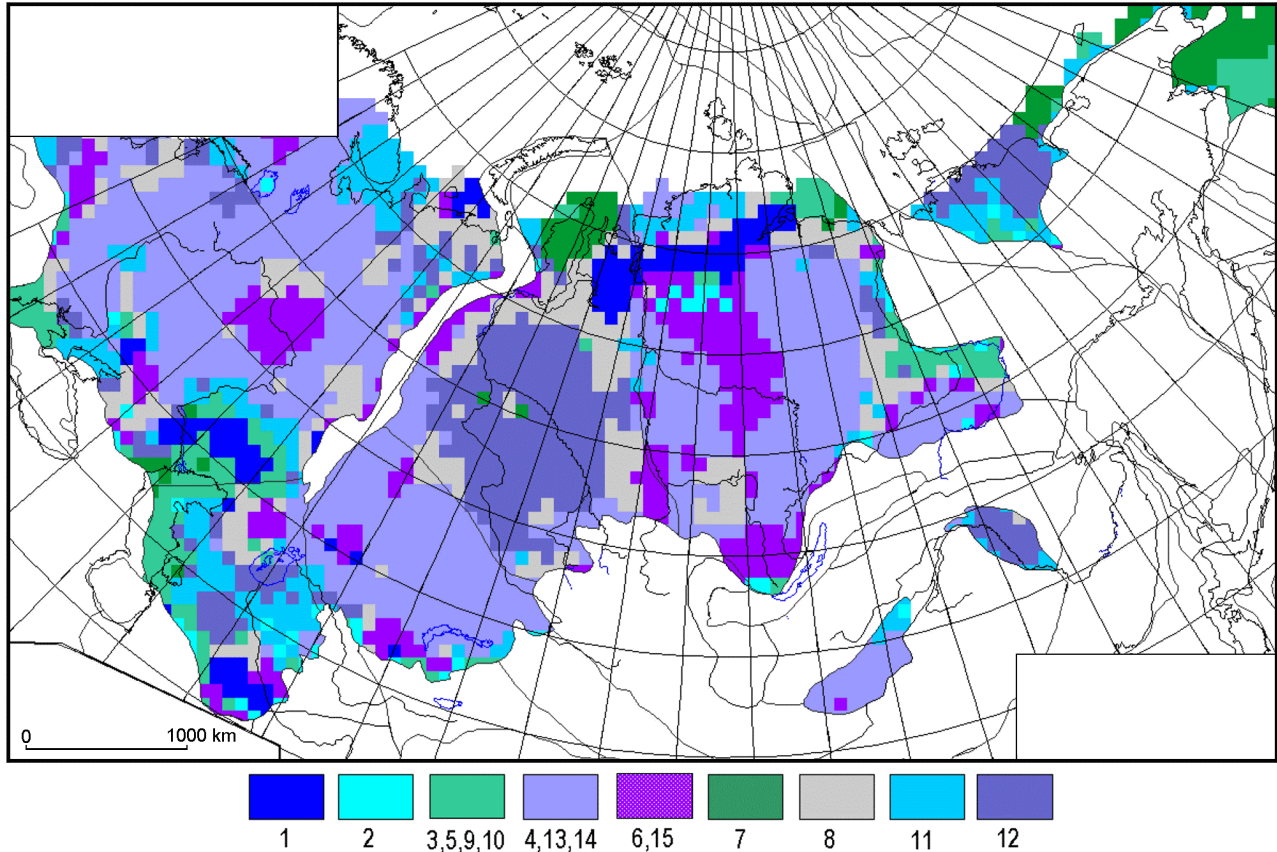


Figure 17. Classification of platform areas. 9 classes derived from three factors.

orogenic regions. It also includes the northern part of the East Asian continental rift, Vitim-Stanovoi prerift area and southern part of the Moma rift.

Classes 4 and 6, united in accordance with the dendrogram, include the Carpathians and the Pannonian basin, Sakhalin, Kamchatka, Eastern Chukotka, and the Indol-Kuban trough in the Caucasus. Class 7 is represented by only 73 cells and is developed in the Eastern Caucasus and in some parts of the Central Tien Shan. Class 8 occupies 419 cells and includes the Rioni basin in the Caucasus, in Kopet Dag, on the northern and southern slopes of the Fergana basins, and in the westernmost part of the Verkhoyansk-Kolyma orogenic system. Class 9 is noticeable in the Fergana basin, Kura basin, Baikal rift and, incoherently, Moma rift. Class 10 consists of 526 cells and is developed in the Trans-Caucasian region, the Pamirs, the South Tien Shan, Dzhungaria and the East Sayany prerift area. Class 12 consists of 126 cells and is mostly developed in the Northern Caucasus. Class 14, comprising 172 cells, is mainly observed in the Tien Shan.

Assessing the inferred results of the geodynamic regionalization of entire North Asia and comparing the scheme of neotectonic geostructural regions (Figure 1) with the geody-

namic regionalization scheme (Figure 19), we arrive at the following conclusions.

(1) Heterogeneity of platform regions is clearly recognizable. One should primarily note a distinction between ancient and young platforms, which is basically important because the notions of ancient and young platforms involve essentially tectonic meaning [Shatsky, 1964]. The fact that geophysical parameters resolve the difference between these types of platforms is of crucial significance for geodynamics as regards deep structural features.

(2) As is evident from Figure 19, significant heterogeneities are observable within ancient and young platforms. The well-defined central area of the epi-Paleozoic West Siberian plate is associated with the system of buried rifts at the base of the platform cover, being recognizable as a zone of lower P wave velocities [The Russian Arctic..., 2002]. This area is surrounded by lithospheric blocks of high P wave velocities that can be interpreted as "paleoarms" of the Early Mesozoic rift system of the West Siberian plate.

It is interesting that the northernmost part of this area around the Ob River mouth, where the continental crust was broken up by rifting and the Ob paleocean was developed [Aplonov, 1988], is observed in the geodynamic re-

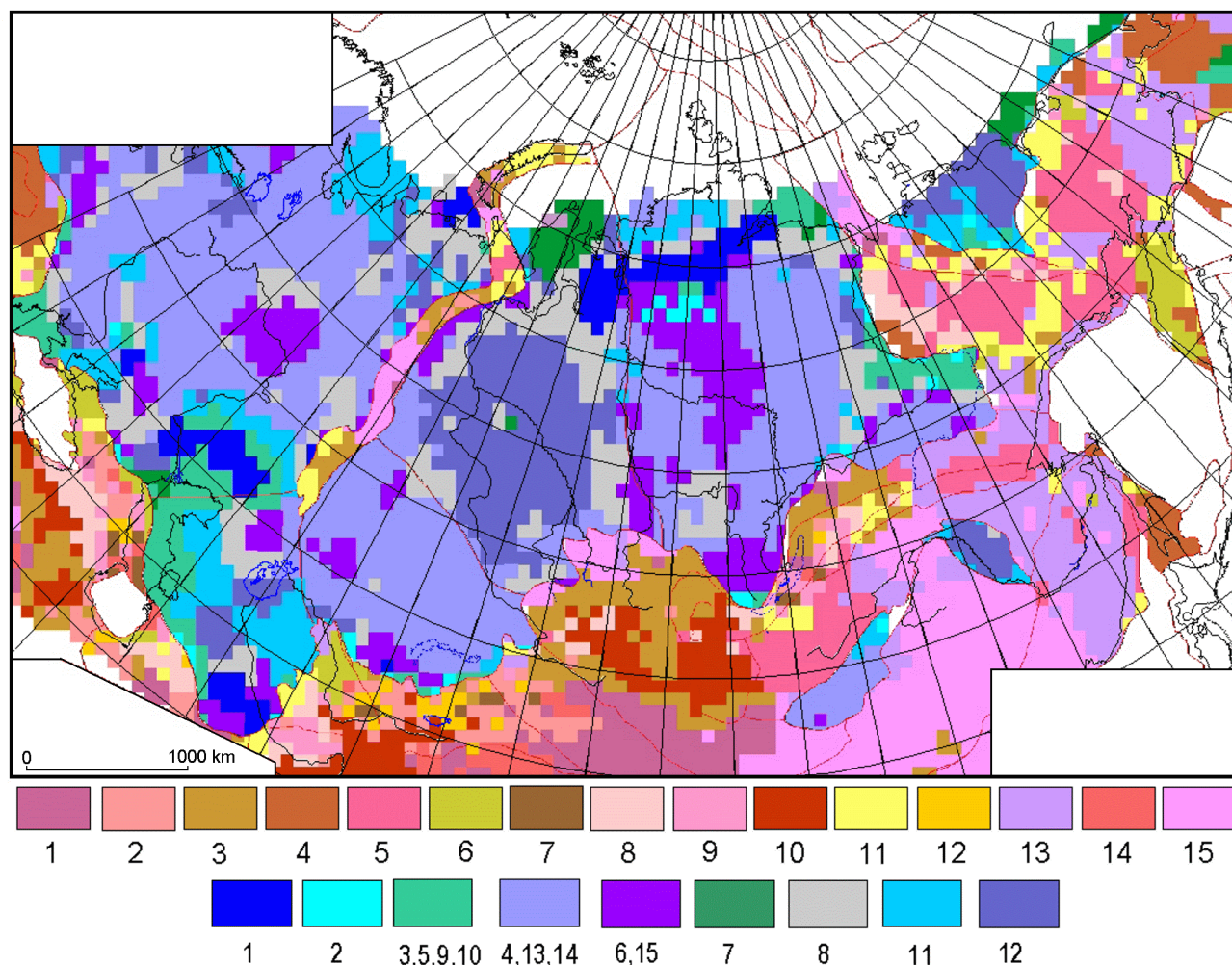


Figure 18. Map of geodynamic zoning of Northern Eurasia (see explanation in text).

gionalization map as a distinct zone protruding into the Kara Sea (Figure 19). Another young platform, the Turan plate, is also strongly heterogeneous: at least three areas differing in the lithosphere structure are recognizable here [Neotectonics..., 2000].

Heterogeneities within ancient platforms are also well-expressed. The north- and southeastern boundaries of the EEP observable as two reentrant angles are noteworthy. These are the Timan-Pechora basin in the northeast and the Cis-Caspian syncline in the southeast. The latter includes a well-visible structural bench that reflects an abrupt drop in the depth to basement and is similar to the bench observed at the transition from the Taimyr fold zone to the East Siberian platform.

Also well-expressed are density inhomogeneities within ancient platforms: anomalous areas related to trap magmatism are observed in the East Siberian platform and in the Voronezh Massif of the EEP. In both cases, one may expect that further studies will reveal in these areas the presence

of a high-velocity layer in the lower crust associated with an underplating process.

(3) Even more contrasting heterogeneities are observed in active regions of North Eurasia. Thus, the Middle Urals separating the North and South Urals is distinguished in the weak orogeny structure of the recent Urals. Based on comparative analysis of the regional Urals-Appalachian types, such a subdivision was suggested previously [Grachev, 1967], when data were deficient. This conclusion is of undoubted interest in relation to the discussion on the tectonic origin of the Urals at the neotectonic stage.

Highly contrasting heterogeneities are observed in the orogenic belt of the Central Asia, where the structures of the Pamiro-Alai, South and North Tien Shan, and Tarim basin are fairly well resolved (cf. Figures 1 and 19). A prifiting area involving part of the Tunkin rift is distinguished in Mongolia. A similar area is recognizable within the Kyrgyz and Chinese Tien Shan and adjacent part of the Tarim basin.

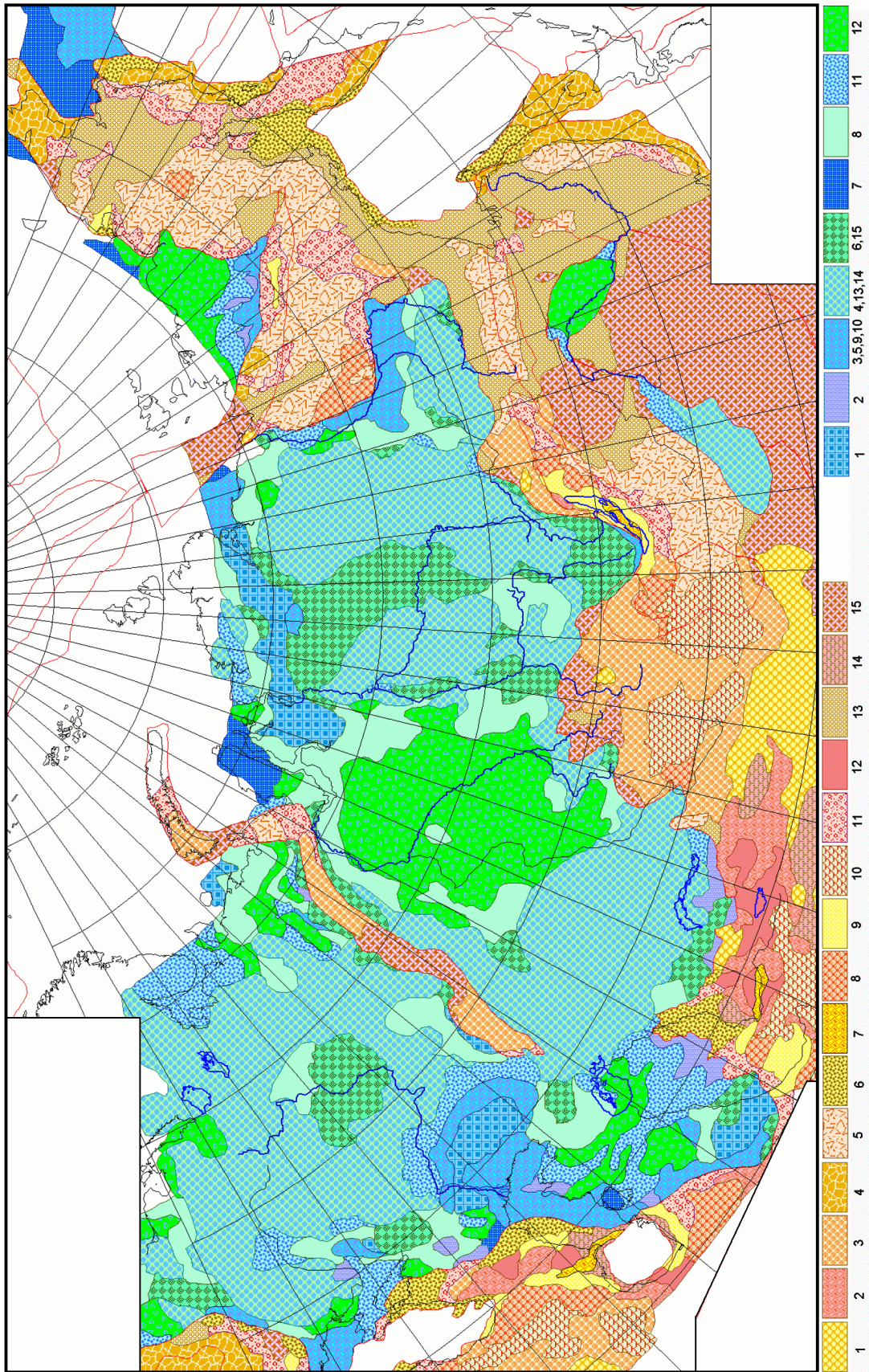


Figure 19. Same as Figure 18, smooth boundaries between classes.

The Baikal rift zone, considered as a coherent neotectonic structure, is strongly heterogeneous, which largely related to the heterogeneity of the basement on which the rift developed. Contrasts are highest in its northeastern part, including the Muya and Chara rift valleys and surrounding mountainous structures.

Naturally, detailedness of the geodynamic regionalization scheme, for the first time constructed for the entire territory of North Eurasia, is primarily determined by initial data, and in certain regions these data are obviously inadequate (for example, in northeastern Asia). For this reason, results of these study should be considered as a first approximation to those of future investigations based on an updated and wider dataset.

References

- Aplonov, S. A. (1988), Mesozoic paleogeodynamics of the West-Siberian plate, in *Main problems of geotectonics*, pp. 154–161, Nauka, Moscow.
- Artemjev, M. E., V. I. Bune, V. A. Dubrovsky, and N. Sh. Kambarov (1972), Seismicity and isostasy, *Phys. Earth Planet. Inter.*, 6(4), 256–262.
- Artemjev, M. E., and M. K. Kaban (1994), Density inhomogeneities, isostasy and flexural rigidity of the lithosphere in the Transcaspian region, *Tectonophysics*, 240, 281–297.
- Artemyev, M. E., V. E. Golland, and G. A. Niauri (1985), New data on the isostasy of the Caucasus, *Phys. Solid Earth*, 21(2), 85–93.
- Artemyev, M. E., A. P. Belov, M. K. Kaban, and A. I. Karaev (1992), Isostasy of the lithosphere of Turkmenia, *Geotectonika*, 26(1), 48–58.
- Artemjev, M. E., M. K. Kaban, V. A. Kucherinenko, G. V. Demjanov, and V. A. Taranov (1994), Subcrustal density inhomogeneities of Northern Eurasia as derived from the gravity data and isostatic models of the lithosphere, *Tectonophysics*, 240, 249–280.
- Assameur, D. M., and J.-C. Mareshal (1995), Stress induced by topography and crustal density heterogeneities: implication for seismicity of southeastern Canada, *Tectonophysics*, 241, 179–192.
- Davis, J. C. (1973), *Statistics and data analysis in geology*, 571 pp., New York.
- Feng, E., V. Cermak, R. Haenel, and V. Zui (1996), *Geothermal atlas of Europe*, Hermann Haack, Verlagsgesellschaft.
- Grachev, A. F. (1967), Tectonic development of the weak orogeny regions, *Tectonic movements and neotectonic structures of the crust*, pp. 69–74, Nedra, Moscow.
- Grachev, A. F. (2nd Ed.) (1987), *Rift Zones of the Earth* (in Russian), Nedra, Moscow.
- Grachev, A. F. (2000), The Pannonian rift, in *Neotectonics, Geodynamics and Seismicity of North Eurasia* (in Russian), pp. 171–185, Probel, Moscow.
- Grachev, A. F., and V. O. Mikhailov (1988), On the origin of intraplate sedimentary basins of an isometric shape, in *Intraplate Phenomena in the Earth's Crust* (in Russian), pp. 159–166, Nauka, Moscow.
- Grachev, A. F., V. A. Magnitsky, and I. V. Kalashnikova (1986), Recent and Late Cainozoic geodynamics of the Central Europe, in *Abstracts, 7th Int. Symposium on Recent Crustal Movements of the Earth*, pp. 48–49, Tallinn.
- Grachev, A. F., V. A. Magnitsky, and I. V. Kalashnikova (1987a), Recent crustal movements, neotectonics and physical fields in the Carpathian–Balkan region: Analysis of neotectonic sedimentation and volcanism, *Fiz. Zemli* (in Russian), (8), 3–20.
- Grachev, A. F., V. A. Magnitsky, and I. V. Kalashnikova (1987b), Recent crustal movements, neotectonics and physical fields in the Carpathian–Balkan region: Composition and state of the upper mantle and the origin of recent and neotectonic activity, *Fiz. Zemli* (in Russian), (9), 3–15.
- Grachev, A. F., N. K. Frolova, Sz. Sz. Grigorjan, et al. (1987c), The Specification of Geological Position and Nature of the Fault in the Paks NPP District, Manuscript, Paks Atomeromu Rt., Foldrenges Proekt Jelentestara, Paks.
- Grachev, A. F., V. A. Magnitsky, and I. V. Kalashnikova (1988), Recent crustal movements and neotectonics of the Pannonian basin, in *6th Int. Symp. "Geodesy and Physics of the Earth," Abstracts*, pp. 31–32, Potsdam.
- Grachev, A. F., V. A. Magnitsky, I. V. Kalashnikova, and I. L. Lapushonok (1989), Recent crustal movements in relation to seismicity in the Pannonian basin, *Fiz. Zemli* (in Russian), (9), 3–8.
- Grachev, A. F., I. V. Kalashnikova, and V. A. Magnitsky (1990), Recent crustal movements and seismicity, *Fiz. Zemli* (in Russian), (11), 3–12.
- Grachev, A. F., V. A. Magnitsky, V. O. Mikhailov, and T. V. Romanyuk (1992), Geodynamic evolution of the Pannonian basin: Synthesis of geological and geophysical data and numerical modeling, in *Abstracts. Int. Symp.*, Moscow.
- Grachev, A. F., V. A. Magnitsky, Sh. A. Mukhamediev, and S. L. Yunga (1995a), Tensor characteristics of recent bending deformations and basement surface curvatures of the East European platform, *Dokl. Ross. Akad. Nauk* (in Russian), 340, 250–255.
- Grachev, A. F., V. A. Magnitsky, Sh. A. Mukhamediev, and S. L. Yunga (1995b), Tensor characteristics of neotectonic bending deformations and basement surface curvatures of the East European platform, *Dokl. Ross. Akad. Nauk* (in Russian), 340, 389–395.
- Grachev, A. F., V. A. Magnitsky, and V. A. Nikolaev (2001a), Interpretation of data on recent crustal movements in the Pannonian basin, *Dokl. Ross. Akad. Nauk* (in Russian), 381, 532–535.
- Grachev, A. F., V. A. Magnitsky, and V. A. Nikolaev (2001b), Recent crustal movements in the Pannonian basin and the problem of their interpretation, *Izvestiya, Phys. Solid Earth*, 37, 987–994.
- Hurtig, E., V. Cermak, R. Haenel, and V. Zui, (Eds.) (1992), *Geothermal atlas of Europe*, 1st ed., Hermann Haack Verlagsgesellschaft.
- Kaban, M. K. (2001), A gravity model of the North Eurasia crust and upper mantle: 1. Mantle and isostatic residual gravity anomalies, *Russian J. Earth Sci.*, 3(2), 125–144.
- Kaban, M. K. (2002), A gravity model of the north Eurasia crust and upper mantle: 2. The Alpine-Mediterranean foldbelt and adjacent structures of the southern former USSR, *Russian J. Earth Sci.*, 4(1), February.
- Kaban, M. K. (2003), Density inhomogeneities in the upper mantle, lithosphere isostasy and geodynamics, Doctoral (phys.-math.) dissertation, Inst. Phys. Earth. Russ. Acad. Sci., Moscow.
- Kaban, M. K., and M. E. Artemjev (1993), The Density Lithosphere structure of the Eastern Europe and Its Relation to Tectonics, *Terra nova, Abstr. suppl. (EUG VII, Strassburg)*, 5(1), p. 54.
- Kaban, M. K., and S. L. Yunga (2000), On the influence of the density inhomogeneities to the stress field and seismicity of the Baikal rift, *Russ. Acad. Sci. Reports*, 371, pp. 527–531.
- Kaban, M. K., and P. Schwintzer (2001), Oceanic upper mantle structure from experimental scaling of V_s and density at different depths, *Geophys. J. Int.*, 147, 199–214.
- Kaban, M. K., M. E. Artemjev, A. I. Karaev, and A. P. Belov (1998), The deep structure and geodynamics of the tectonic features in Turkmenistan and adjacent areas; gravity evidence, *Geotectonika*, 32(4), 323–332.
- Khain, V. E., and N. V. Koronovsky (1997), Caucasus, in *Encyclopedia of European and Asian regional geology*, Collection: Encyclopedia of Earth sciences series, Fairbridge-Rhodes-W (editor), 127–136.
- Kostyuchenko, S. L., A. V. Egorkin, and L. N. Solodilov (1999),

- Structure and genetic mechanisms of the Precambrian rifts of the East-European Platform in Russian by integrated study of seismic, gravity, and magnetic data, *Tectonophysics*, 313(1-2), 9-28.
- Lithospheric dynamics atlas of China* (1989), 225 pp., China Cartographic Publishing House, Beijing.
- Mukhamediev, Sh. A. (1992), The lithosphere bending as a cause of certain seismotectonic features, *Reports of Academy of Sciences USSR*, 324(5), 986-989.
- Neotectonics, geodynamics and seismicity of North Eurasia* (in Russian) (2000), 498 pp., Probel, Moscow.
- Nikolaev, V. A. (2000a), Relation of seismicity to cutvstures of new tectonic deformations of the crust in northern Eurasia, *Third meeting of Asian Seismological Commission (an affiliation to the IASPEI) and Symposium on Seismology, Earthquake hazard assessment and Earth's interior related*, p. 74, Tehran, I.R. Iran.
- Nikolaev, V. A. (2000b), Gradients of neotectonic crust movements in the Northern Eurasia, *Matireals of XXXIII Tectonic conference "General problems of tectonic, Tectonic of Russia"*, pp. 112-114, MGU, Moscow.
- Nikolaev, V. A. (2001), Neotectonic and geodynamic of East-European platforms, *Tectonic of neogei: General and regional aspects*, Vol. 2, pp. 78-79, Materials of XXXIV Tectonic conference, Moscow.
- Nikolaev, V. A. (2002), Geodynamic regionalization of the East European platform, in *Tectonics and Geophysics of the Lithosphere* (in Russian), vol. 2, pp. 56-58, Geos, Moscow.
- Ritzwoller, M. H., A. L. Levshin, L. I. Ratnikova, and A. A. Egorkin (1998), Intermediate-period group-velocity maps across Central Asia, western China and parts of the Middle East, *Geophys. J. Int.*, 134, 315-328.
- The Russian Arctic: geological history, mineragenesis, environmental geology* (2002), 958 pp., St.Petersburg.
- Trubitsyn, V. P. (2000), Principles of the tectonics of floating continents, *Izvestiya, Phys. Solid Earth*, 36, 708-741.
- Trubitsyn, V. P., and V. V. Rykov (2000), A 3-D spherical model of mantle convection with floating continents, U.S. Geological Survey, *Open File Rep. 00-218*, pp. 2-44.
- Zoback, M. L. et al. (1992), World stress map - maximum horizontal stress orientation, *J. Geophys. Res.*, 97(B8).

A. F. Grachev, M. K. Kaban, and V. A. Nikolaev, Schmidt United Institute of Physics of the Earth, Russian Academy of Sciences, Bol'shaya Gruzinskaya ul. 10, Moscow, 123995 Russia

(Received 22 January 2004)